HOLOCENE CLIMATE VARIABILITY, VEGETATION DYNAMICS AND FIRE REGIME IN THE CENTRAL PYRENEES: THE BASA DE LA MORA SEQUENCE (NE SPAIN)

A. Pérez-Sanz (1), P. González-Sampériz (1), A. Moreno (1), B. Valero-Garcés (1), G. Gil-Romera (1), M. Rieradevall (3), P. Tarrats (3), L. Lasheras-Álvarez (1), M. Morellón (2), A. Belmonte (4), C. Sancho (4), M. Sevilla-Callejo (1), A. Navas (5)

1) Instituto Pirenaico de Ecología (IPE)-CSIC. Avda. Montañana 1005, 50059 Zaragoza, Spain

2) Instituto de Geociencias, CSIC,UCM. José Antonio Nováis, 2, 3ª planta, 3b. Facultad de Ciencias Geológicas, Univ. Complutense. 28040 Madrid, Spain.

3) Grup de Recerca F.E.M. (Freshwater Ecology and Management) and IRBio (Institut de Recerca de Biodiversitat) Departament d'Ecologia. Fac de Biologia. Univ. de Barcelona Av. Diagonal 643, 08028 Barcelona, Spain.

4) Departamento de Ciencias de la Tierra. Univ. de Zaragoza. C/ Pedro Cerbuna s/n. 50009 Zaragoza, Spain

5) Estación Experimental de Aula Dei (EEAD)-CSIC. Avda. Montañana 1005, 50059 Zaragoza, Spain

ABSTRACT

High resolution multiproxy data (pollen, sedimentology, geochemistry, chironomids and charcoal) from the Basa de la Mora (BSM) lake sequence (42º 32' N, 0º 19' E, 1914 m a.s.l.) show marked climate variability in the central southern Pyrenees throughout the Holocene. A robust age model based on 15 AMS radiocarbon dates underpins the first precise reconstruction of rapid climate changes during the Holocene from this area. During the Early Holocene, increased winter snowpack and high snowmelt during summer, as a consequence of high seasonality, led to higher lake levels, a chironomid community dominated by non-lacustrine taxa (*Orthocladiinae*) related to higher inlet streams, and a forested landscape with intense run-off processes in the watershed. From 9.8 to 8.1 cal ka BP, climate instability is inferred from rapid and intense forest shifts and high fluctuation in surface run-off. Shifts among conifers and mesophytes reveal at least four short-lived dry events at 9.7, 9.3, 8.8 and 8.3 cal ka BP. Between 8.1 and 5.7 cal ka BP a stable climate with higher precipitation favoured highest lake levels and forest expansion, with spread of mesophytes, withdrawal of conifers and intensification of fires, coinciding with the Holocene Climate Optimum. At 5.7 cal ka BP a major change leading to drier conditions contributed to a regional decline in mesophytes, expansion of pines and junipers, and a significant lake level drop. Despite drier conditions, fire activity dropped as consequence of biomass reduction. Two arid intervals occurred between 2.9-2.4 cal ka BP and at 1.2-0.7 cal ka BP (800-1300 AD). The latter coincides with the Medieval Climate Anomaly and is one of the most arid phases of the Holocene in BSM sequence. Anthropogenic disturbances were small until 700 AD, when human pressure over landscape intensified, with *Olea* cultivation in the lowlands and significant deforestation in highlands. Colder and unfavourable weather conditions during the second part of the Little Ice Age caused a temporary cease of high-land management. The most intense anthropogenic disturbances occurred during the second half of 19th century. Last decades are characterized by recovery of the vegetation cover as a result of land abandonment, and lowered lake levels, probably due to higher temperatures.

Key words: Holocene; central Pyrenees; climate evolution; vegetation history; palaeohydrology; fire; abrupt changes.

1.- INTRODUCTION

Long-term climate evolution during the Holocene has been strongly modulated by orbitally-forced insolation trends which determine heat distribution throughout the planet. In the northern Hemisphere, summer insolation sets limits on the position and strength of the Inter Tropical Convergence Zone (ITCZ), which controls the position of the north-hemisphere cell atmospheric system (Wanner and Brönnimann et al. 2012). In particular, the location of the Azores High and the Iceland Low pressure centres determines the latitudinal position and intensity of the North Atlantic westerlies and the storm tracks, which largely govern rainfall distribution in the Western Mediterranean area (Greatbatch, 2000, Marhsall et al. 2002). During the Early Holocene, the maximum summer insolation in the Northern Hemisphere led to a rapid northward displacement in the ITCZ and its associated rain belt (Fleitmann et al., 2007). This northern position of the ITCZ was responsible for bringing moisture to the current world-largest desert in North Africa (Sahara and Sahel) (deMenocal et al., 2000). As the summer insolation decreased the ITCZ displaced southward, the monsoon system weakened and in south-western Europe the climate followed a general trend to an increasingly aridity since the Mid Holocene that led to decreased lake levels (Magny et al., 2007, 2011; Valero-Garcés and Moreno, 2011) and major shifts in the vegetation composition (Fletcher and Zielhofer, 2011; Roberts et al., 2011).

However, beyond this general climate trend, many recent studies have documented the existence of rapid climate variability during the Holocene (Bond et al., 1997, 2001; Mayewski et al., 2004). Although the nature and mechanisms of these abrupt climate changes still remain unclear, weakening in the thermohaline circulation as consequence of meltwater inputs in the North Atlantic has been recognised as one of the most important triggers (Renssen et al., 2007; Wanner et al., 2008). Furthermore, fluctuations in solar activity have also been responsible for climate shifts (Wanner et al., 2011). These short-living episodes of climate variability had a large impact over most of Europe, as it has been recorded in many continental palaeoclimate archives as lacustrine sediments (Magny et al., 2007), glacial deposits (Davis et al., 2009), and pollen records (Bordon et al., 2009; Magyari et al., 2012).

Holocene climate reconstructions for the North Atlantic region involve mainly changes in temperature (Brooks and Birks, 2001). However, in the Mediterranean area Holocene variability is mostly related to changes in water availability as it is

86 documented in vegetation distribution (Jalut et al., 2009; Sadori et al., 2011), lake levels
87 (Magny et al., 2011) and stalagmite growth (Fleitmann et al., 2007; Spötl et al., 2010).
88 The Iberian Peninsula climate integrates subtropical, Mediterranean and Atlantic
89 influences due to its geographical location between the Mediterranean Sea and the
90 Atlantic Ocean (Lionello et al., 2006). Moreover, the Iberian Peninsula has proven to be
91 particularly sensitive to short-term climate shifts during the Holocene (Moreno et al.,
92 2012a). Lakes experienced noteworthy variations in response to precipitation and
93 evaporation shifts during the Holocene (Valero-Garcés et al., 2000; González-Sampériz
94 et al., 2008; Martín-Puertas et al., 2008; Morellón et al., 2009). Changes in sea surface
95 temperatures (Cacho et al., 2001) and deepwater formation (Frigola et al., 2007) in the
96 Western Mediterranean show a fast response to changes in the North Atlantic. Other
97 Iberian continental records highlight a large Holocene variability. For example, the
98 isotope record in the Kaite Cave stalagmite (Domínguez-Villar et al., 2008) reflects
99 variations in the amount of precipitation related to North Atlantic dynamics and
100 fluctuations in palaeoflood activity of Tagus River, in Central Spain have been related
101 to changes in prevailing atmospheric circulation patterns (Benito et al., 2003). Although
102 vegetation is a very good indicator of past climate variability, there are only a few high-
103 resolution pollen studies from the Iberian Peninsula (e.g. Fletcher et al., 2013a,
104 Jiménez-Moreno and Anderson, 2012), documenting the fast response of vegetation to
105 abrupt climate changes (decadal- to centennial-scale) during the Holocene.
106 A recent study has proved the high-sensitivity of middle-latitude high mountain
107 ranges in general, and the Pyrenees in particular, to current global warming,
108 documenting an speeding up of replacement of cold-adapted plants by thermophilic
109 species (Gottfried et al., 2012). Past climate changes during the Holocene should have
110 also affected the flora and landscape of the Pyrenees. Furthermore, the southern slopes
111 of the Pyrenees are not affected by Foehn winds, and the present climate is rather
112 complex, influenced by a progressive west-to-east decrease in precipitation, due to
113 weakening of the Atlantic humid fronts inland. Thus, the southern Pyrenees experience
114 both Atlantic and Mediterranean climate regimes within a relatively short distance of
115 less than 450 Km. The Pyrenean vegetation reflects these climate conditions, varying
116 from humid-Atlantic forests, dominated by oak and beech, in the west, to Mediterranean
117 forests, dominated by pine and drought-resistant taxa, in the central and eastern regions.
118 Due to these particular geographical features the Central Pyrenees play a key role in
119 providing information about past E-W shifts of the boundary between both regimes as a

result of shifts in the atmospheric components and, particularly, shifts in the westerlies strength.

In Western Europe, human disturbances in the landscape can be traced back to the Neolithic period and the climate signal is often masked by anthropogenic activities during the most recent times (Oldfield, 2005; Carrión et al., 2007). Discriminating anthropogenic from natural forcings in landscape evolution has been subject of much debate during recent years. High-altitude sites are more useful than low-altitude sites for detecting climate signals, since more inhospitable climate conditions limit intense human landscape intervention.

Here we present a paleo-environmental reconstruction of climate, vegetation and fire dynamics from a lacustrine sequence located in the central part of the southern Pyrenees: the Basa de la Mora sequence. This record stands out as one of the best climate archives to tackle questions concerning: i) how the Atlantic and Mediterranean regimes have progressed along the Holocene, ii) identification of rapid episodes of climate change, and iii) elucidation of high mountain land-use system during recent times.

2.- STUDY AREA

2.1 Geological and geomorphological setting

Lake Basa de la Mora (BSM) (42º 32' N, 0º 19' E, 1914 m a.s.l.) is a small, shallow glacial lake located on the north-facing slope of the Cotiella Peak (2912 m a.s.l.), the highest summit of the Cotiella Massif in the central southern Pyrenees (Fig.1a). The Cotiella Massif belongs to the homonymous nappe, located in the western part of the South Pyrenean Central Unit (Seguret, 1972).

The landscape surrounding the lake results from intense karstic and glacial activity. Lake Basa de la Mora occupies a glacial over-deepened basin enclosed by a frontal moraine (Belmonte, 2004) and surrounded by steep limestone walls. The catchment consists of Mesozoic limestones and sandy limestones affected by several thrust sheets (reverse faults). Triassic marl and evaporite formations crop out at the base of the thrust sheets, providing a hydrological seal for the lake and favouring localized surface drainage into the lake along some creeks. Triassic ophite formations in the watershed are the source of highly characteristic sediments (hematite and other Fe- mineral with high magnetic susceptibility) within the lake deposits.

The Basa de la Mora basin belongs to the watershed of the Cinca River, one of the main tributaries of the Ebro River. The lake has smooth margins, a relatively small watershed (209 ha) and a total lake surface of ca. 3 ha. It is characterized by large seasonal water-level fluctuations: the maximum depth varies from ca. 2.5 to 4.5 m seasonally. The lake is fed by precipitation, surface runoff, ephemeral creeks and several small springs located on the southern margin. Water losses take place through a surface outlet to the north and evaporation. The substrate, made up of non-permeable Triassic material, greatly restricts groundwater losses.

2.2.- Climate and vegetation

The Pyrenees is a mountain range in south-western Europe that extends from the Atlantic Ocean in the west to the Mediterranean Sea in the east, leading to a diverse climate and plant community along a W-E transect. The precipitation in the Pyrenees results from two different mechanisms: precipitation in the east is linked to cold fronts, while precipitation in the west comes from Atlantic frontal systems (Millán et al., 2005). The Atlantic influence extends as far as the Ordesa Valley (García-Ruiz et al., 2001), ca. 150 km from the Atlantic coast and 22 km west of the BSM. Both systems

are directly related to the North Atlantic Oscillation (NAO) that principally determines precipitation in western Europe (Trigo et al., 2002).

The climate of the study area is sub-Mediterranean with continental features. Rainfall (annual average = 1360 mm) peaks during spring and autumn, following the Mediterranean pattern (García-Ruiz et al., 1985). However, summers are not as dry as is typical of the Mediterranean because of frontal and convective precipitation which affects the mountainous areas in July and August. Mean air temperatures range from 0.5 to 15ºC between the coldest (January) and warmest (July) months, respectively.

The vegetation cover shows a characteristic contrast between south and north facing slopes: the southern slopes are characterised by mediterranean-type components with sclerophyllous shrubland and evergreen *Quercus* communities, while the northern slopes have mixed conifer/deciduous taxa forests, including *Pinus sylvestris*, *Pinus uncinata*, *Abies alba*, *Betula alba*, *Corylus avellana*, *Fagus sylvatica*, *Quercus faginea* and *Quercus petraea* (Fig. 1b).

The elevational gradient between the valley bottoms and the Cotiella Peak, from 550 to 2900 m a.s.l., gives rise to an altitudinal distribution of vegetation, typical of mountain environments. Lowlands are occupied by crops and valley bottoms by riparian corridors (*Fraxinus excelsior*, *Populus* spp., and *Salix* spp.). Forests occur from the base of the foothills up to ~ 2000 m a.s.l. Below 1700 m a.s.l., the dominant species are determined by moisture availability and temperature range, mostly controlled by the slope orientation. From 1700 to 2000 m a.s.l. the forest is mainly composed of *Pinus uncinata* mixed with *Juniperus communis* shrubland and *Rhododendron ferrugineum* at the treeline. Above 2000 m a.s.l., steep rock formations and harsh climate prevent forest development, leading to a scrub-dominated landscape formed by dwarf junipers (*Juniperus communis sbsp. nana*), and alpine grassland (*Nardus stricta, Festuca eskiae, Caricion davallianae* and *Cynosurus cristatus*). Lake Basa de la Mora (BSM) is located in the subalpine belt, near the treeline, so the vegetation surrounding the lake is alpine grassland, *Pinus uncinata* forest and *Juniperus communis-Rhododendron ferugineum* shrublands.

3.- METHODOLOGY

The composite sequence of Basa de la Mora (BSM08-1A-1U) is based on two parallel cores retrieved from the deepest part of the lake in summer 2008. The longest core was taken with an Uwitec coring system and platform from the Pyrenean Institute of Ecology (IPE-CSIC). Two gravity cores were taken to recover the uppermost part of the sequence and the sediment/water interface. One of the short cores (BSM08-1A-1G) was sub-sampled every 1 cm in the field for ^{210}Pb and ^{137}Cs analyses and the other core (BSM08-1B-1G) was used to complete the upper part of the sequence. The cores were correlated applying sedimentological and geochemical criteria. The total length of the composite sequence is 12.10 meters. An additional littoral core (BSM-2A-1U) was taken in order to compare lacustrine depositional environments.

The cores were split lengthwise into two halves, imaged with a DMT Core Scanner and analyzed with a Geotek Multi-Sensor Core Logger (MSCL) at 5 mm intervals to characterise the sediment physical properties at the Limnological Research Center at the University of Minnesota (USA). Elemental geochemical composition was analyzed using the Itrax XRF Core Scanner at the Large Lakes Observatory (LLO) at the University of Minnesota (USA) at 0.5 cm resolution using 30-s count times, 30 kV X-ray voltage, and an X-ray current of 20 mA. These measurements provide estimates of relative element concentrations. The cores were sub-sampled at 2 cm resolution for Total Organic Carbon (TOC) and Total Inorganic Carbon (TIC) and analysed with a LECO144DR elemental analyser at the IPE-CSIC laboratory of Zaragoza (Spain). Sedimentary facies were defined by macroscopic characteristics including colour, grain-size, sedimentary structures, fossil content and by microscopic smear slide observations (Schnurrenberger et al., 2003) (Fig. 3). The sedimentological descriptions are supported by Scanning Electronic Microscopic (SEM) observations of selected samples made at the University of Zaragoza (Spain). Up to 11 samples representing the main facies were analysed for grain size distributions using a Malvern Laser Sizer (Mastersizer 2000) after removing the organics by H_2O_2 and using a dispersant agent to disaggregate the samples. Additionally, 36 samples were analysed for their mineralogical content by X-Ray Diffraction using an automatic Siemens D-500 X-ray diffractometer: Cu ka, 40 kV, 30mA and graphite monochromator. Identification and quantification of the different mineralogical species present in the crystalline fraction were carried out following a standard procedure (Chung, 1974). Sedimentary facies and physical properties (density, magnetic susceptibility) were also obtained for the littoral core (BSM-2A-1U).

Samples for pollen analyses were obtained every 5 cm on both the BSM08-1A-1U and BSM08-1B-1G cores. This record covers the whole sedimentary record, except the base of the sequence (1209 - 1165.5 cm depth) which was samples at higher resolution (1 cm) since the sedimentation rate was extremely low (see below). Sediment samples were prepared following the standard protocol described by Faegri and Iversen (1964) or Moore and Webb (1978), with some modifications (Dupré, 1988) includeg HCl, and KOH and HF digestion, mineral-organic particles separation with Thoulet solution (2.0 gr/cm^3 density) and sieving with 212 and 10µm mesh. *Lycopodium* spores in a known concentration were added in order to calculate the pollen concentration in the sediment and to test the laboratory procedures (Stockmarr, 1971). Pollen was identified using an optical microscope, with help of the reference collection of the IPE-CSIC and identification keys (Moore et al., 1991; Reille and Lowe, 1995). Counts were made to obtain a pollen sum, excluding aquatics and exotics, of at least 300 grains from a minimum of 20 taxa. The results have been plotted using PSIMPOLL 4.27 (Bennett, 2009).

Correlation analyses were made on smoothed data, after testing for normality (Shapiro-Wilk), using Pearson or Spearman correlation tests. Analysis have been performed by the R software package (Venables et al., 2008), Pairwise comparison was performed between MS and geochemical parameters, to help in the facies description, and then between MS (as a high-resolution sedimentological proxy) and the pollen data, to assess possible links between sedimentary changes and vegetation.

Sedimentary micro-charcoal particles were identified on pollen slides by optical microscopy. Only charcoal particles over 10 µm were counted and these were easily identified as black, angular and opaque particles (Clark, 1988). Charcoal influx (mm^2/cm^3) was estimated after Tinner and Hu (2003). No *Lycopodium* spores were found in some of the slides, so charcoal influx values were obtained by linear interpolation between the adjacent samples.

Chironomid samples were collected every 20 cm along the entire core, except at the top of the sequence (2.5-50 cm depth) where the sample interval was increased to 5 cm. The samples were processed following the standard procedure (Hofmann, 1986): 10% KOH digestion at 70º and 300 rpm for 20 minutes, followed by sediment sieving (90 µm). *Chironomidae* larvae head capsules were examined under stereo microscope using a Bolgorov tray, picked out manually and dehydrated in 96% ethanol, before being mounted ventral side upwards in Euparal® as permanent slides. Taxonomic

identification was carried out using an optical microscope (Olympus CX41) at 40x magnification and Cell B Imaging Software for Life Science Microscopy (Olympus). The larval head capsules were identified to the lowest taxonomic level possible using several specialized guides (Wiederholm, 1983; Rieradevall and Brooks, 2001; Brooks et al., 2007).

The chronology of the sequence is based on 15 calibrated AMS radiocarbon dates from the long core BSM08-1A-1U and ^{137}Cs and ^{210}Pb dating from the short core BSM08-1B-1G (Fig. 2). Most of radiocarbon dates are based on terrestrial macrofossils and charcoal (Table 1). Bulk sediment and pollen concentrates were dated in the lowermost part of the sequence because of the paucity of organic remains. Dates have been calibrated using CALIB 6.0 software and the INTCAL09 curve (Reimer et al., 2009). The 2σ probability distribution interval was chosen. The age model was constructed by linear interpolation between the median ages of the probability distribution of adjacent calibrated dates. The $^{210}Pb_{ex}$ and ^{137}Cs activity in the upper samples was measured by gamma-ray spectrometry, using a high-resolution low-energy coaxial HPGe detector coupled to an amplifier. The chronology based on $^{210}Pb_{ex}$ was estimated by applying the constant rate of supply (CRS) model by Appleby (2001). The resulting age model provides a robust chronological framework for the high resolution paleo-environmental reconstruction presented in this work.

4.- RESULTS

4.1.- Chronology

According to the age-depth model, the BSM sequence spans the last ca. 16 cal ka BP (Table 1, Fig. 2). The two lowermost dates (at 11.98 and 12.06 m depth) are the only ones not based on terrestrial macrofossils (Table 1). When these two dates are included in the age model (12628 ± 100 and 15828 ± 600 cal yr BP), they result in a change from consistently high sedimentation rates (1.2 mm/yr) between 0-11.67 m depth to extremely low rates (0.064 mm/yr) at the base (11.67-12.09 m depth). Given that these dates point out to the Late Glacial period, we attempted to characterize this zone by increasing the pollen sampling. However, the pollen record did not show changes indicative of the last glacial-interglacial transition (LGIT, see section 4.3, zone BSM-0). Since there is no sedimentary evidence for a depositional hiatus, and no major change in the vegetation composition has been recorded, these two dates were not used in the final age model. It is possible that a reservoir effect is responsible for these samples being too old. The age model excluding the two basal dates indicates that the 11.67 m long record spans the last ca. 9.8 cal yr BP (Fig. 2). The final age-depth model is based on 13 calibrated AMS radiocarbon dates, 11 on macrofossils and two on charcoal. The short core, that includes the most recent period, has been dated by ^{210}Pb and ^{137}Cs activities. Two well-defined ^{137}Cs peaks are recorded at the uppermost part of the sequence providing markers for the 1954-1959 and the 1963 maximum atmospheric nuclear bomb testing. The chronology based on $^{210}Pb_{ex}$ compares fairly well with the ^{137}Cs peaks (Fig. 2).

4.2.- Sedimentary facies, geochemistry and lithological units

Six sedimentary facies were identified based on visual description, microscopic observations, grain-size data and mineralogical and geochemical composition (Table 2). The sediments consist of either: i) carbonate – poor (< 2 % TIC), with lower TOC and high MS, organized in laminated or banded intervals, or ii) carbonate-rich (2 – 7 % TIC) with variable, but higher organic matter content (1-3 %) and low magnetic susceptibility, arranged in massive to banded deposits. The grain-size data indicates finer (mode at 6-7 μm) and better-sorted sediments in the silicate-rich, carbonate- poor facies, and coarser and more poorly sorted material in the carbonate-rich sediments.

The first group of sediments (Facies 1, 2 and 3) are banded to laminated silicate and carbonate fine silts dominated by clay minerals (20-30 %) and quartz (5-15 %) with minor amounts of calcite (< 25 %) and with presence of hematite, pyrite and

clinochlorite. Facies 3 has the highest MS, and relatively high carbonate content. Facies 1 and 2 are more silicate-rich, but Facies 2 is finer, with lower MS, better-defined lamination and higher TOC content than Facies 1. The second group (Facies 4, 5 and 6) is dominated by massive carbonates (ca. 6% TIC; 60-80% calcite). Facies 5 and 6 have mottled textures and abundant gastropods, indicating littoral deposition. These facies dominate the littoral core (BSM-2A) almost entirely. Facies 4 has a higher TOC content (up to 3%) dominated by macrophyte and terrestrial remains. Facies 5 contains authigenic crystals of carbonate and gypsum, partially dissolved, pointing to deposition in ephemeral lake conditions with rapid fluctuations of lake level and salinity. Diatoms (pennate, benthic) only occur in the carbonate-rich Facies 5. Facies 6 has a slightly banded texture and lower TOC content than the other carbonate facies.

The BSM sequence has been divided into three main sedimentary units according to sedimentary facies, MS, TIC and TOC percentages and the mineralogical and geochemical composition (XRF) (Fig. 3).

i) Unit 3 (1168-491 cm depth; 9800-5700 cal yr BP) corresponds to the lowermost part of the sequence and it is characterized by banded carbonate – poor sediments with high values of MS and relatively low TOC percentages (Facies 1, 2 and 3). TIC percentages and Ca, Sr and S values are low throughout Unit 3 while Si, K, Ti values (and particularly Fe and Mn) are high. The lowermost Sub-unit 3b (1168-690 cm depth, 9800-7450 cal yr BP) is composed of laminated Facies 1 and a thin interval of Facies 3. Magnetic Susceptibility (MS) reach the highest values of the sequence and are positively correlation with Mn (Table 3a). The high MS values are related to the presence of paramagnetic minerals eroded from ophite outcrops. Values of Ca and TIC are relatively low, but also display a strong positive correlation with MS. TOC percentages are the lowest in the sequence while TOC/N ratios are the highest. Sub-unit 3a (690-491 cm depth, 7450-5700 cal yr BP) is composed of Facies 2 and has finer lamination, lower MS and higher TIC and TOC values. Sub-unit 3a MS values are still high but decrease progressively. MS is significantly positively correlated with Mn and Fe (Table 3a). Ca values are very low and not significantly correlated with MS. TOC percentages increase, showing a significant negative correlation with MS, while TOC/N ratios decreases.

ii) Unit 2 (491-93 cm depth; 5700-680 cal yr BP) is made up of carbonate-rich Facies 5 and 6 with intercalations of organic-rich Facies 4. Thus, Unit 2, although

highly variable, is characterized by the lowest values of MS and the highest content in TIC of the whole sequence. The high values of TIC in Unit 2 (up to 8%) are related to precipitation of authigenic carbonates. Sr and S elements increase considerably in this unit. TOC percentages also vary greatly during this period but, in general, they are relatively high and increase upwards. Relatively low TOC/TN values (< 12) indicate the dominance of lacustrine organic matter (Meyers, 2003). Si, Ti, Fe and Mn show parallel trends to MS (Table 3a). Unit 2 can be subdivided into three sub-units, following the facies association. Thus, *BSM 2c* (491-350 cm depth; 5700-3540 cal yr BP) is constituted by the alternation of cm-thick intervals of Facies 4 and 6 and displays an upward TIC increase (up to 8%). TOC percentages are highly variable but generally low (1-2 %). *BSM 2b* (350-240 cm depth; 3540-2200 cal yr BP) represents a 1 m-thick interval of Facies 5 with the highest TIC, Ca and calcite values and the lowest TOC and MS of the sequence (Fig. 3). Higher Sr values occur as a result of more abundant biogenic aragonite. Finally, *BSM 2a* (240-93 cm depth; 2200-700 cal yr BP) comprises rhythmic sequences of about 20 cm-thick composed of thin layers of Facies 1->, Facies 4 -> Facies 5 (detrital- organic-carbonate).

iii) Unit 1 (93-0 cm depth; 698 cal yr BP-2007 AD) comprises carbonate – poor Facies 1 and organic-rich Facies 4. As a consequence, all geochemical indicators show high variability. Facies 1 lamination is less well defined than in Unit 3. MS values increase again and show strong positive correlation with Si, Ti, Mn and Fe, while the correlation with Ca and TIC and TOC is strongly negative (Table 3a). TOC/N ratios increase at the base of the unit and decrease towards the top: TOC percentages show the opposite pattern.

4.3. Pollen and charcoal data

The pollen record can be divided into six zones (BSM-0 to BSM-V: Fig. 4). In BSM-I to BSM-V (9.8 ka cal BP-present), the 5 cm-resolution pollen analyses provide a temporal resolution of 22 to 150 years per sample.. Statistical results for pairwise comparison between vegetation and geochemical parameters are shown in Table 3b. The maximum number of charcoal particles counted was 3098, with a mean of 307 and a SD of 453. The patterns of charcoal influx are consistent with the pollen zones.

BSM-0 (1209-1167.5 cm depth; before 9800 cal yr BP)

This zone is characterised by scarce representation of the herbaceous component (NAP) and particularly the steppe taxa group (*Artemisia*, *Chenopodiaceae, Helianthemum, Plantago, Rumex*, which rarely exceed 5-10 %), and abundanbt representation of arboreal pollen (AP), dominated by conifers (mainly *Pinus*) and deciduous forest taxa (*Betula*, *Corylus*, *Alnus*, *Salix*, *Ulmus*, *Populus*, *Acer*, *Fraxinus*, *Fagus*, *Tilia* and deciduous *Quercus*), with values around 25-30 % (Fig. 4)., Representation of Poaceae and aquatics (Cyperaceae, *Ranunculus, Myriophyllum* and *Potamogeton*) in this zone is not significantly different to the rest of the sequence. This pollen spectrum is not consistent with a pre-Holocene deposit as would be inferred from the two dates (15.8 cal ka BP and 12.6 cal ka BP) from this interval. These spectra, together with the lack of sedimentological evidences for a hiatus, indicate that these dates are too old. Both pollen and sedimentological data suggest these are Holocene sediments, but given the absence of chronological control the record from this zone is not considered further in this study.

BSM-I (1167.5-815 cm depth; 9800-8200 cal yr BP)

Arboreal pollen varies between 60 and 80% of the total pollen abundance, and in some cases it exceeds 85%. *Pinus* is the main arboreal taxon, but deciduous taxa are well represented by *Betula*, *Corylus* and deciduous *Quercus,* with some significant fluctuations in *Betula*. *Juniperus* is also present with percentages above 6%. Evergreen *Quercus* and Mediterranean shrubs (*Pistacia*, *Rhamnus*, *Phillyrea*, *Buxus*, *Sambucus*, *Ephedra fragilis* and *E. distachya*) are present in relatively low but continuous percentages. The first *Tilia* is recorded at 870 cm depth (8500 cal yr BP); this timing is consistent with other records from the region (Montserrat-Martí 1992; González-Sampériz et al., 2006; Miras et al., 2007; Pèlachs et al., 2007). Poaceae dominates the herbaceous stratum, while the abundance of *Helianthemum* significantly declines and *Artemisia* decreases in importance. *Myriophyllum* is the dominant aquatic. A significant change is found towards at the end of the zone (860 - 815 cm depth; 8400-8200 cal yr BP) characterized by a sharp decline in *Betula*, *Corylus* and deciduous *Quercus*, the virtual disappearance of Other Mesophytes (Fig. 4) and the total absence of *Tilia*. *Pinus* increases to its maximum in the whole sequence, reaching 75%, and *Helianthemum* reappears at this time. This is a phase of high variability in fire activity, although charcoal counts are very low. *Pinus* and *Juniperus* show apositive correlation with MS within this zone, while *Betula*, *Corylus*, *Quercus faginea*, evergreen *Quercus* and

Myriophyllum are negatively correlated with MS (Table 3b). Thus, MS is correlated negatively with moisture-adapted and temperate taxa, but positively with more drought-resistant taxa such as *Pinus* and *Juniperus*.

BSM-II (815-491 cm depth; 8200-5700 cal yr BP)

After the short, abrupt vegetation change previously described, forest contracts slightly but there is considerable compositional variability. *Pinus* decreases to 35% and *Juniperus* is also highly reduced in abundance. Deciduous taxa, mainly *Betula*, *Corylus* and deciduous *Quercus,* show large and more continuous expansion reaching their maximum values in the sequence. *Tilia* reappears and is constantly present at moderate levels throughout the zone. Evergreen *Quercus* declines to its minimum values, while Mediterranean Shrubs fluctuate in abundance. The first isolated appearance of *Abies* occurs at 646 cm (7200 cal yr BP). The NAP is mainly composed by *Poaceae*, *Artemisia* and Lamiaceae, as in the rest of the record. Aquatic plants are well represented by Cyperaceae, *Pedicularis, Ranunculus* and *Potamogeton,* although *Myriophyllum* is dominant and reaches its highest values in the sequence. Deciduous *Quercus* and *Tilia* abundances show a strong negative correlation with MS (Table 3b). There is an increasing trend of fire activity, although the variability is high.

BSM-III (491-389 cm depth; 5700-3900 cal yr BP)

The beginning of this zone is characterized by a steep decline in deciduous forest taxa, mainly *Betula (*abruptly reduced by nearly 60%) and deciduous *Quercus*. In contrast, *Pinus* expands rapidly and *Juniperus* and evergreen *Quercus* increase slightly. *Fagus* appears for the first time, chronologically fitting the regional expansion (Montserrat-Martí, 1992; Pla and Catalán, 2005). The base of the zone is characterised by the permanent presence of *Abies* in the area, after its initial appearance shortly before. Poaceae, *Artemisia,* Lamiaceae and Chenopodiaceae are still the main NAP taxa and *Rumex* rises. No significant changes are recorded on the aquatic component except a decrease in *Myriophyllum* and a short-term disappearance of *Potamogeton* at the base of the zone. The conifer/mesophyte ratio is inverted at the top of the zone, just before the transition from Sub-unit 2c into Sub-unit 2b. Fire activity reaches a maximum towards the end of this zone.

BSM-IV (389-93 cm depth; 3900-700 ca yr BP)

The beginning of this zone is characterized by a change in forest composition. *Pinus* recovers and becomes the dominant arboreal taxon, *Abies* reaches its maximum abundance and *Betula* exhibits its minimum values. *Juniperus* and evergreen *Quercus* increase, but *Corylus* and Other Mesophytes only experience a slight increase. *Tilia* decreases progressively and disappears at top of the zone. In contrast, *Fagus* reaches its highest levels, at a time consistent with other records from the region (Pla and Catalán, 2005; Pérez-Obiol et al., 2012). A sudden and abrupt rise of *Artemisia* and further decrease in mesophyte taxa accompany the *Pinus*-dominant landscape. The NAP, of which Poaceae and *Artemisia* constitute the main elements, accounts for 40% of the pollen sum. There are two peaks of *Artemisia* in this zone, the youngest of which (when *Artemisia* reaches its maximum value in the whole sequence) coincides with the disappearance of *Abies* and *Tilia*. The aquatic component is markedly reduced in abundance, with low values of *Myriophyllum* and the absence of *Potamogeton* during the most of the zone contrasting with an increase in Cyperaceae. Cultivated taxa like *Olea*, *Vitis*, *Castanea* and *Cerealia* type appear more continuously. Although there are some marked peaks of *Pinus* in this zone, the general trend is for relatively stable pine forest during the last phase of sedimentary Sub-units 2b and 2a. An abrupt decrease in charcoal concentration lasting several centuries was followed by a new abrupt increase in fire activity at the end of the zone.

BSM-V (93-0 cm depth; 700 cal yr BP-present, 1250-2008 cal AD)

This zone is characterized by important changes in both pollen and sedimentological records (Unit 1). The most relevant feature is the increase in *Olea* and *Fraxinus*. *Pinus* increases up to the 70%, but with very short episodes of were abundance is much lower (40%). The expansion of pine is coincident with the decline of *Abies*, *Betula, Corylus* and Other Mesophytes. Deciduous *Quercus* and, especially evergreen *Quercus* increase in abundance in the topmost part of the sequence. The NAP is still dominated by Poaceae, but *Artemisia* drops dramatically while Asteraceae and Chenopodiaceae reach their maximum values. *Myriophyllum* becomes less important and Cyperaceae dominates the aquatic assemblage. Variations in MS at this time are not correlated with vegetation composition changes. Fire activity is very high during most of the zone, but ceases in the top part of the record.

4.5. Chironomids

A total of 6422 chironomid head capsules were picked up, individually mounted and identified from 71 samples of the core BSM08-1A. Total chironomid biodiversity was represented by 18 taxa (up to 9 taxa per sample), belonging to three chironomid subfamilies: *Tanypodinae, Orthocladiinae* and *Chironominae. Tanytarsus* gr. *lugens* was the most abundant all through the core, followed by *Procladius*, *Chironomus* and *Paratanytarsus*,. *Chironomus* or *Paratanytarsus* are not shown in the diagram (Fig. 5) because they are present through the entire sequence and show no clear pattern of changes through the Holocene. The chironomid assemblage indicates that the lake has been always relatively shallow and oligotrophic, although relatively rich in organic matter. Quantitative analysis of the *Chironomidae* allows the sequence to be divided into 4 zones:

CHZ-1: Chironomid Zone 1 (1168.5-491 cm depth; 9895 - 5700 cal yr BP)

Low densities characterize this zone. *Tanytarsus* gr. *lugens* abundance is relatively low although with some fluctuations. *Procladius* reaches its maximum relative abundance within the core (30-60%), whereas *Pentaneurini* tribe appears through the entire zone although with a highly fluctuating distribution. The *Orthocladiinae* tribe is quite diverse, with an early representation of *Psectrocladius* gr. *limbatellus* and *Corynoneura* and a moderate representation of *Orthocladiinae* indet. (5-7%), which include several taxa related to water runoff and seepages (e.g. *Smittia*).

CHZ-2: Chironomid Zone 2 (491-357 cm depth; 5700 - 3600 cal yr BP)

The *Tanypodinae* subfamily taxa (*Procladius* and *Pentaneurini*) is reduced in abundance, whereas the abundance of *Tanytarsus* gr. *lugens* increase and remains relatively high values throughout the zone (50-60%). Density values increase, although 3 samples from the base of the zone were almost sterile.

CHZ-3: Chironomid Zone 3 (357-56 cm depth; 3600 - 350 cal yr BP)

High densities occur, although they decrease towards the top of the zone. The main difference from the previous zone is the presence of *Psectrocladius* gr. *limbatellus* throughout the zone with relatively high abundances (up to 20%). *Procladius* reaches relatively high abundance (10-20%), although it does not reach previous values.

CHZ-4: Chironomid Zone 4 (56-0 cm depth; 350 cal yr BP - present; 1600 - 2008 AD)

The uppermost zone is characterized by a strong increase of *Psectrocladius* gr. *limbatellus,* together with *Pentaneurini* and *Corynoneura,* and a reduction in *Tanytarsus*

524 gr. *lugens*. Density values particularly of *Procladius,* fluctuate, although its abundance
525 is similar to the previous zone.
526

5. DISCUSSION

5.1. The Early Holocene: Strong Mediterranean influence and high climate variability (Sub-unit 3b, BSM-I, CHZ 1, 9800-8150 cal yr BP)

During the Early Holocene, the Atlantic regions of Iberia were dominated by deciduous broadleaf trees (Muñoz-Sobrino et al., 2005, 2007; Moreno et al., 2011) while the Mediterranean, mountain and inland areas were covered mainly by dense pine forest (Carrión et al., 2010; Franco-Múgica et al., 2000; Rubiales et al., 2010 Morales-Molino et al., 2012). The southern Pyrenees record both climate regimes in a relative small area: the Atlantic climate to the west and the Mediterranean climate to the east. These particular geographical features led to some marked differences in plant communities between the two regions at the onset of the Holocene. Increasing humidity was much pronounced in the Atlantic-influenced area, with a large expansion of mesophytes (Montserrat-Martí 1992; González-Sampériz et al., 2006), while pine was the main tree taxon in the Mediterranean-influenced region (Miras et al., 2007; Pérez-Obiol et al., 2012). This suggests a stronger W-E precipitation gradient in the southern Pyrenees at the onset of the Holocene, with stronger influence of humid fronts in the west and persistent summer drought in the east.

In the BSM sequence, located at the modern transition between the Atlantic and Mediterranean climate regimes, the Early Holocene is characterized by the dominance of conifers over mesophytes (BSM-I) (Fig. 5). High values of pines and *Juniperus* reflect a continental Mediterranean-climate influence during this period. The fire regime is not characterised by either frequent or virulent fires, probably because of fuel limitation as pine-dominated forests are less flammable than broadleaf woodlands. The dominance of *Pinus* over deciduous taxa suggests the existence of extreme seasonal temperatures and marked summer drought during the Early Holocene. However, deposition of carbonate-poor laminated Facies 1 and 3 indicates permanent and relatively high lake levels with abundant sediment delivery by run-off. High values of MS are related to the presence of paramagnetic minerals eroded from ophite outcrops and are consistent with high-energy transport to the lake. High correlation between MS and Ca and TIC is indicative of the detrital origin of carbonate minerals and supports high erosion rates during this period. The high abundance of non-lacustrine *Orthocladiinae* taxa, related to inlet streams, in this zone supports the idea of increased runoff due to high rainfall. The *Procladius* genus has been reported to be important in

561 the Early Holocene in other European regions (Heiri et al., 2003) and its high abundance
562 is consistent with higher lake levels because it inhabits fine sediments in the profundal
563 zones of lakes (Saether, 1979; Prat et al., 1992).
564 The Early Holocene maximum in seasonality in the Northern Hemisphere may
565 have been responsible for particularly cold winters and hot summers. In the southern
566 Pyrenees, this would have led to increased snow accumulation in winter and subsequent
567 large snowpack melt during the warmer summer months leading to higher run-off.
568 Evapotranspiration and low precipitation during summer drought periods would be
569 largely compensated by increased melting water, leading to higher lake levels. The
570 negative correlation between moisture-adapted taxa and MS supports the idea that run-
571 off would be likely linked to melt processes rather than direct precipitation.
572 Furthermore, positive correlation between MS and drought-resistant taxa such as
573 *Juniperus* and *Pinus* confirms that run-off is related to increased continentality during
574 this period.
575 The relatively dry and cold Early-Holocene climate of the Basa de la Mora (BSM)
576 is in agreement with many studies from western Europe (Leira and Santos, 2002; Bjune
577 et al., 2005;) and North America (Shuman et al., 2001; Zhao et al., 2010), which have
578 inferred a cooler and drier climate probably related to weakened ocean conveyor
579 circulation as the rapid, global increase in temperature provoked large input of
580 freshwater from the Laurentide sheet into the North Atlantic, weakening Labrador Sea
581 deep convection (Kaplan and Wolfe, 2006; Renssen et al., 2009, 2012).
582 Superimposed on the long-term insolation-driven climate trend, the BSM
583 sequence shows significant short-term (submillennial) shifts in pollen percentages and
584 sedimentological features during the Early Holocene. Such shifts occurred at 9.7, 9.3,
585 8.8 and 8.3 cal ka BP and are mainly characterized by short-term expansion of pine,
586 accompanied by large reductions in all deciduous taxa but most particularly in *Betula*,
587 implying a substantial reduction in humidity. The highest MS values of the whole
588 sequence are also recorded during these events, indicating that these periods are
589 characterised by particularly intense run-off and sediment delivery from the catchment
590 (Fig. 5). Cold and relatively humid winters with large amount of snow accumulation,
591 and the subsequent snowpack melt and runoff, could be responsible for increased
592 erosion in the catchment. This interpretation is supported by the sharp and
593 discontinuous presence of rheophilous and non-strictly lacustrine chironomid taxa
594 during these short-events. Low percentages of TOC and low TOC/N ratio also point to

595 reduced vegetation in the catchment (Fig. 5). Phases of reduced forest may be due to a
596 downward displacement of the treeline, supporting the occurrence of cooler
597 temperatures. These events were as short-lived periods of drier and cooler conditions.
598 Sedimentary phases with particularly high sedimentation rates associated with arid
599 conditions have been recognised in the Central Ebro Basin complex during this period
600 (Sancho et al., 2008; Gómez-Paccard et al., 2013). The strong response of the vegetation
601 and hydrology at BSM indicates that climate instability was characteristic of the Early
602 Holocene. Similar evidences for Early Holocene climatic oscillations have been widely
603 recognised throughout the North Atlantic region (O´Brien et al., 1995; Alley et al.,
604 1997; Mayewski et al., 2004; Bond et al 1997, 2001; Frigola et al., 2007).
605 The first Early Holocene cold event is recorded just at the beginning of the BSM
606 sequence at 9.8-9.7 cal ka BP. Since the BSM record starts at 9.8 cal yr BP, we suggest
607 that this may be coincident with the short-lived 9.95 ka cold anomaly detected in the
608 NGRIP record (Rasmussen et al., 2007). The impact of this anomaly has been
609 previously noted in the western Mediterranean as a phase of forest decline (Fletcher et
610 al., 2010b), as in BSM sequence. A global event centred in 9.3 ka cal BP has been
611 widely recorded in many sequences from the North Atlantic and Europe (Haas et al.,
612 1998; Rasmussen et al., 2007; Fletcher et al., 2013b). In the BSM sequence, this interval
613 coincides with an expansion of pine forest and decline in mesophyte taxa but there is no
614 sedimentological change. The next cold and arid event occurs at 8.8 ka cal BP. In BSM
615 sequence, this event is resulted in major shifts in vegetation and sediment deposition
616 and the apparent disappearance of chironomids. This phase coincides with the only
617 occurrence of Facies 3 and the high TOC/TN ratios characteristic of this unit suggest a
618 well-vegetated watershed, dominated by *Pinus*. The 8.8 ka cal BP cool event is reported
619 in the Artic by Ebbesen et al., (2007) but has not previously been reported in southern
620 Europe.
621 The next event is recorded at 8.3 ka cal BP. This is the most remarkable
622 vegetation shift in the BSM record, with *Pinus* reaching its highest values and *Betula*
623 dropping to its minimum. Taking into account the age-depth model uncertainties for this
624 period (8300 ± 100 cal yr BP), this event could be synchronous with the 8.2 ka cool
625 event (Alley and Agustsdottir, 2005; Rasmussen et al., 2007), triggered by a large
626 freshwater discharge from former glacial Lake Agassiz into the North Atlantic Ocean,
627 causing a reduction the Atlantic Meridional Overturnign Circulation (AMOC) (Hoffman
628 et al. 2012). The high-resolution study carried out in BSM sequence for this period

indicates a minimum timing of 150 years and maximum of 200 years for the 8.2 ka event. This timing agrees with the precise characterization of the 8.2 ka event obtained from trapped air in a Greenland ice core (GISP2) (Kobashi et al. 2007). The abrupt increase in pine in BSM matches the spread of *Pinus* recorded in the Alps (Blarquez et al., 2009), Switzerland (Tinner and Lotter, 2001) and northern Spain (Muñoz Sobrino et al., 2007), suggesting a widespread impact in mountain/alpine regions. The 8.2 event is widely recorded in the north-eastern of the Iberian Peninsula, where human settlements located in a particular harsh region of the Central Ebro basin moved towards more humid areas during this interval (González-Sampériz et al., 2009).

The rapid response of the vegetation to these short climate shifts, related to changes in the North Atlantic, seems to be amplified in the BSM sequence because of its ecotonal location for some species. The highly responsive nature of the vegetation record highlights the climate sensitivity of high altitude transitional areas to environmental changes, as previously demonstrated for the central Pyrenees during the Lateglacial period in El Portalet sequence (González-Sampériz et al., 2006).

5.2. The Mediterranean "Climatic Optimum" (Sub-unit 3a, BSM-II, CHZ-I, 8100-5700 cal yr BP)

The Mid-Holocene is the period with the greatest forest development in Europe, when treeline moved upward and reached its maximum elevation in most mountain regions (David 1993; Ali et al.2003; Ortu et al., 2008; Carnelli et al., 2004; Favilli et al., 2010; Talon et al., 2010; Cunil et al., 2011; Magyari et al., 2012). In northern Europe, forest expansion is related to higher summer temperature (Davis et al., 2003; Bjune et al., 2005; Nesje et al., 2006), while in southern Europe this is an interval of increased humidity (Carrión et al., 2010; Colonese et al., 2010; Spötl et al., 2010; Stoll et al., submitted).

There is a marked shift in the vegetation composition after ca 8.2 ka BP in the BSM sequence, (Fig. 5). *Betula*, *Corylus* and deciduous *Quercus* became the dominant AP elements, *Tilia* and other mesophytes were present, and conifers declined to their minimum values, with pine oscillating between 20-30 % and juniper between 2-3% (Fig. 5). This assemblage is very different from that of a dense conifer community near the lake (Court-Picon et al., 2005). The high values of *Betula* (up to 26%) in the BSM sequence compare fairly well with similar high values recorded in the Pyrenean sequence of El Portalet peatbog (González-Sampériz et al., 2006), located at 1802 m

663 a.s.l, Lake Burg (Pèlachs et al., 2007), located at 1821 m a.s.l. or Tramacastilla lake, at
664 1682 m a.s.l., where birch accounted for 40% of the total pollen (Montserrat-Martí,
665 1992). The similarity between these sequences indicates that *Betula* grew at higher
666 altitude, in the upper part of the montane belt and probably reaching the subalpine belt.
667 The rise of birch and the consequent drop of pine at BSM could result from either an
668 increase in annual precipitation or reduced evaporation, as a consequence of decreased
669 continentality, favouring water-demanding taxa. High charcoal values indicate increased
670 regional fire activity. An increase in moisture does not necessarily imply reduced fire
671 activity; the expansion of mesophytes, which are more flammable than most mountain
672 pines (Blarquez and Carcaillet, 2010), provides high amounts of fuel at an altitudinal
673 zone normally devoid of large forest to be burnt. Only minimal changes in summer
674 climate or lightning would be required to promote large and virulent fires, leaving a
675 sizeable imprint in the charcoal record. In addition *Betula* is a pioneer taxa that spreads
676 well after fire disturbances (Blanco, 1997; Morales-Molino et al., 2012). This pattern
677 has been also found in El Portalet sequence (Gil-Romera et al., submitted) and in many
678 other Holocene records from the European mountains (Tinner et al., 1999; Colombaroli
679 et al., 2008; Vannière et al., 2008) as well as in current patterns of fire occurrence
680 (Pausas and Paula, 2012).
681 The interval from 8100-5700 cal yr BP was characterized by stable environmental
682 conditions in the BSM catchment, as inferred from the stable vegetation composition
683 and the lack of marked decreases in any tree taxon despite the high fire activity.
684 Sedimentological and geochemical indicators indicate a stable, relatively deep lacustrine
685 environment. The laminated nature of Facies 2 is consistent with high lake level and the
686 activity of several inflow streams. The finer grain size of Facies 2, in comparison to
687 laminated Facies 1 and 3, indicates even higher lake levels. Low values of TIC and Ca
688 suggest dilute water, and the lack of a significant correlation between Ca and MS
689 indicates that delivery of carbonates from the catchment through run-off was negligible.
690 Moreover, the decrease in MS and TOC/N along with the increase in TOC suggests a
691 more vegetated environment that would limit the erosive effect of precipitation. High
692 and constant *Myriophyllum* values and the chironomid association also reflect a well-
693 established, deeper lacustrine environment; as genus *Procladius* presents its highest
694 abundances along the sequence and *Tanytarsus* gr. *lugens* is also important in the
695 chironomid assemblage. Moreover, the increase of littoral and macrophyte-related taxa
696 such as *Corynoneura* or *Pentaneurini* tribe (e.g. Brodersen et al., 2001) during this

period, reflects the greater development of aquatic vegetation in the lake favored by milder climate conditions.

The Mid-Holocene warmer conditions occurred when the flux of meltwater from the Laurentide ice sheet stopped and deep convection in the Labrador Sea led to enhanced transport heat over the Atlantic-influenced area (Renssen et al., 2009, 2012). Increased meridional circulation in the North Atlantic as the Laurentide sheet waned could bring warmer condition to the Iberian Peninsula. Changes in the SST and shifts in insolation triggered reorganization of the atmosphere circulation and strengthened meridional atmosphere circulation. A northward shift of the monsoon system and its associated rainfall belt gave rise to particularly humid conditions in the Sahara and Sahel (deMenocal et al., 2000; Hély et al., 2009). Enhanced westerlies could bring increased summer humidity over the Iberian Peninsula, as inferred from the spread of broad-leaf taxa in this region (Pantaleón-Cano et al., 2003; Carrión et al., 2001, Carrión, 2002).

Although this interval (8.2-5.7 cal ka BP) is the most humid period recorded at BSM,, high MS and a slight expansion of *Pinus* indicates a short-lived arid event around 7.5 cal ka BP. However, mesophytes only decrease slightly suggesting this interval was less pronounced than in previous arid intervals. This event is broadly coincident with the arid 7.4 event detected in southern Spain (Jalut et al., 2000) that has been related to the emergence of the Neolithic in southern Iberia (Cortés Sánchez et al., 2012), and also correlates with a phase of forest decline detected in the western Mediterranean (Fletcher et al., 2010a). In the central southern Pyrenees, this phase does not represent a dramatic change in moisture supply and vegetation recovers rapidly.

5.3. The end of the Middle Holocene: transitional phase (Sub-unit 2c, BSM-IV, CHZ-II, 5700-3900 cal yr BP)

The evolution of the landscape in southern Europe from 6 ka (or even earlier) onwards has been widely assumed to be influenced by both climate and human forcings (Oldfield and Dearing, 2003; Vannière et al., 2008; Roberts et al., 2011, Sadori et al., 2011). Many palynological studies show a clear increase of anthropogenic indicators from the Middle Holocene, pointing to an intensification of human activities and a subsequent change in the vegetation composition related to forest clearance for pastures and agriculture fields (Jalut et al., 2009). However, some of these taxa are naturally

found in xeric Mediterranean ecosystems (De Beaulieu et al., 2005) and this makes it difficult to discriminate between climate and anthropogenic forcings. The spread of xeric vegetation across the Mediterranean region during Middle-Holocene does not necessarily imply anthropogenic degradation of the landscape (Collins et al., 2012). In addition, fire activity in Mediterranean areas increased significantly at this time and its impact on vegetation composition has to be taken into consideration (Colombaroli et al., 2007, 2008, 2009; Vannière et al., 2008, 2011). Increased fire activity can result from anthropogenic activities but also reflects the climatic shift towards arid conditions (Carrión et al., 2001a, 2010; Fernández et al., 2007; Fletcher and Sánchez-Goñi 2007; González-Sampériz et al., 2008; Morellón et al., 2008; Jalut et al., 2009; Corella et al., 2010; Anderson et al., 2011). The expansion of heliophytes (like *Artemisia,* Chenopodiaceae, Asteraceae, *Rumex, Plantago,* Poaceae, and Mediterranean taxa similar to *Cerealia*.) observed during this period is favoured by increased fire, increased aridity, and anthropogenic activity. Overall, the complex changes found in Mediterranean areas at the end of the Mid-Holocene are not necessarily related to intense human pressure, but could equally well be explained by the trend towards drier conditions.

There is a sharp change in the vegetation cover and sedimentological features in the BSM sequences at 5.7 cal yr BP. The pollen record in BSM-IV is characterized by a pronounced increase in pine and decrease in mesophytes, mainly *Betula*, in combination with a rise in *Juniperus*, deciduous and evergreen *Quercus* and heliophytes (*Artemisia* and Chenopodiaceae). The replacement of mesophytes by conifers suggests a change from humid to drier conditions or, at least, a significant shift in the seasonal distribution of the precipitation since reduced summer rainfall is unfavourable to the broad-leaf taxa. The sedimentary shift is defined by an increase in carbonates, indicating lower lake levels (Sub-unit 2c). Lower values of MS suggested reduced sediment transport as consequence of lower run-off and inflow streams, which in turn indicates reduced precipitation or meltwater inputs. The decrease in allochthonous sediments is reflected in lowered sedimentation rates and deposition of carbonate Facies 6, which reflects high carbonate productivity in a littoral setting with low and fluctuating water level. The decline in *Myriophyllum* is consistent with a reduction in water level (Figs. 4 and 5). Moreover, the sharp decrease in *Procladius* and the near disappearance of non-lacustrine *Orthocladiinae* taxa also indicates reduced runoff and stream inflow during

this period. The increase in chironomid abundances, mainly *Tanytarsus*, could indicate increased decomposition rates in the sediments.

Both biological and sedimentological indicators are consistent with a trend to increased aridity and a persistent arid phase between 5.6 to 4.6 cal ka PB (Fig. 5). Similar vegetation changes have been recognised in other Pyrenean sequences (Pelachs et al., 2007), in southern Spain (Jiménez-Moreno and Anderson, 2012) and in Mediterranean records (Carrión et al., 2010). Fletcher et al., (2013b) have identified a major phase of deforestation in the Western Mediterranean during this period. The coincidence between lowered lake levels and forest decline supports the idea of climate as the main forcing. A major climate shift has been recognised in many other regions at this time, including the end of wet conditions in the Sahara between 6 and 5.5 cal ka BP (deMenocal et al., 2000; Kröpelin et al., 2008), and lake-level and vegetation changes indictaing drier conditions in eastern North America (Shuman et al., 2001; Zhao et al., 2012; Menking et al., 2012). The similarities in climate changes between such different geographic areas during the Mid-Holocene suggest broad-scale changes in the coupled ocean-atmosphere circulation. This large-scale and synchronous climate shift may be related to changes in global atmospheric circulation. The weakened summer insolation in North Hemisphere led to a southward shift in the Inter Tropical Convergence Zone (ITCZ) and thus, the summer Asian monsoon also weakened considerably (Wanner and Brönnimann, 2012). Readjustment of these two main climatic system drivers led to the establishment of similar conditions to present atmospheric teleconections (ENSO) since ca 5.5 ka (Wanner et al., 2008; Carré et al., 2012; Fletcher and Moreno 2012). Southward movement of the ITCZ favoured southward shift of the sub-tropical North Atlantic high pressure and led to increased summer aridity in the Iberian Peninsula (González-Sampériz et al., 2008; Morellón et al., 2009; Corella et al., 2010; Valero-Garcés et al., 2011; Carrión et al., 2010; Valero-Garcés and Moreno, 2011). As the North Atlantic high-low pressure system moved away, westerlies became weaker and lost their capacity to penetrate inland.

,A change towards wetter conditions is observed in the BSM sequence between 4.5 and 3.9 cal ka BP, marked by increased abundance of mesophytes, and the recovery of *Betula* and deciduous *Quercus* values (Fig. 5). This humid period corresponds well with a phase of increased storm activity recorded in the Gulf of Lion (Sabatier et al., 2012), suggesting stronger and southward migration of the westerlies. However, the total AP decreases during this phase. This reduction of the arboreal pollen in the BSM

sequence occurs at the same time as the first deforestation phase recognised in the Pyrenean sequence of Tramacastilla at ca. 4000 BP (Montserrat-Martí, 1992). However, no other indicator of anthropogenic pressure was found during this period in the BSM sequence suggesting that the vegetation shift was mainly climate driven. The high regional fire activity detected during this period is the culmination of a previous trend. Although there was an initial dry phase when fire occurrence was linked to the presence of pine forest, higher charcoal influx values during this subsequent humid phase are linked with the spread of mesophyte forest. The fact that fire is high during both humid and arid spells, reflects on the one hand more permanent drying conditions than any time before in the Holocene leading to frequent fire-conducive conditions coupled with relatively high fuel availability from mesophyte vegetation, and on the other hand, the strengthening of fire activity during any interval of mesophyte forest expansion when fire-conducive conditions occur.

5.4. The Late Holocene: Aridity Crisis (Sub-units 2b-2a, BSM-VI, CHZ-III, 3700-700 cal yr BP)

Complex societies developed across the Mediterranean during the Late Holocene and human pressure on the landscape intensified and expanded (Carrión et al., 2007, Bal et al., 2011; Finné et al., 2011; Magyari et al., 2012). High altitude palaeoenvironmental records, where anthropogenic activities would have been limited due to both severe weather and difficult access, provide an opportunity to isolate the climate signal influencing vegetation evolution in recent times (Pérez-Sanz et al., 2011).

The BSM sequence reveals a well forested landscape during most of the late Holocene (AP abundance around 70%, BSM-IV), indicating negligible anthropogenic pressure until ca 1150 cal yr BP, when the first evidence of forest management is found. The trend towards increased aridity that started during the Mid-Holocene transition intensified considerably at 3700 cal yr BP. The pollen record (BSM-V) is characterized by a sharp fall of *Betula* and the disappearance of birch from this area. The expansion of conifers (*Pinus* and *Juniperus*, which reaches its maximum proportions of the whole record), indicates a either a reduction in annual mean precipitation or a significant change in the seasonal distribution of precipitation (Franco-Mugica et al., 2000). The *Pinus* expansion in BSM is coeval with an expansion in other high altitude Pyrenean sites (Pèlachs et al., 2011), which suggests it is more likely to be controlled by changed climate than by human action. At ca. 2900 cal yr BP, *Artemisia* starts to spread rapidly

and *Myriophyllum* decreases strongly (BSM-V). Traditionally, the *Artemisia* expansion has been explained by an increase in pastoral activity during the Late Holocene. However, modern values of *Artemisia* rarely reach 2% even though there is moderate pastoral activity in the BSM area. Given that there is no evidence for major deforestation at the time of the *Artemisia* expansion, it seems unlikely that this represents an interval of more intense anthropogenic activity than today. Nor is the *Artemisia* expansion synchronous with the presence of coprophilous fungi, indicative of intensive pastoral land use (López-Merino et al., 2010). This suggests the *Artemisia* expansion at the Basa de la Mora site indicates a climatically-induced expansion of dry steppe. There is evidences for a period of intensified aridity across the Mediterranean at around 2900-2400 cal yr BP (Jalut et al., 2000).

The deposition of carbonate-rich massive Facies 5, characterized by the presence of authigenic calcite crystals, gastropods, pennate diatoms and mottling textures, indicative of bioturbation, provides evidence for lowered lake levels and the development of a larger palustrine area (Fig. 5) at the time of the expansion of dry steppe. Facies 5 characterises most of littoral core BSM-2A-1U, supporting our interpretation of the depositional environment. The presence of partially dissolved authigenic crystals of calcite and gypsum in Facies 5 suggests the lake was ephemeral and may have desiccated at times. The strong negative correlation between MS and TIC indicates that decreased runoff, and thus reduced external water supply into the lake, led to increased concentration of the lake water and authigenic carbonate precipitation. Furthermore, the negative correlation between MS and drought-resistant taxa such us *Pinus* and evergreen *Quercus* and the positive correlation between MS and *Betula* strengthen the link between lack of run-off and precipiation deficit. Intercalation of organic Facies 4 supports the development of a palustrine area with high accumulation of organic matter. In addition, the high percentages of TOC and low TOC/N ratio indicate increased lacustrine productivity, consistent with shallower conditions. This expansion of littoral areas is consistent with the very high abundance of Cyperaceae while *Myriophyllum* values remain relatively unchanged. The higher percentages (up to 20%) of *Psectrocladius* gr. *Limbatellus* than in previous zones also indicates an increase lacustrine productivity, as this genus is associated with productive environments and/or littoral areas with abundance of biofilm primary production on stones or macrophytes (Rieradevall et al., 1999; Brodersen et al., 2001).

There is no charcoal in the BSM between 3.2-1.5 cal ka BP. An interval of two millennia without fire is highly unusual as fire activity is registered in most southern European sequences during this time (Colombaroli et al., 2010; Tinner et al., 2005: Vescovi et al., 2007; Vannière et al., 2008). Arid pulses could prevent forest development at high altitudes and, therefore, limiting charcoal production through fires but, considering the absence of any other clear biotic or abiotic indicators, it seems more likely that the lack of microcharcoal is linked to taphonomical issues affecting charcoal preservation during oxic periods and/or short sub-aerial exposure events (Facies 5).

There is a common pattern to the evolution of vegetation across the Western Mediterranean (including southern Iberia, northern Africa and Italy) during this interval. A general phase of forest decline has been recorded in marine record MD95-2043 from the Alborán Sea between 3.7 and 2.9 cal ka BP (Fletcher et al., 2013b). In Zoñar sequence, low values of AP (< 10%) and an expansion of steppe taxa occurred between 4 – 2.9 cal ka BP (Martín-Puertas et al., 2008). At Sierra de Gádor (Carrión et al., 2003), *Pinus* and evergreen oak expand at the expense of deciduous *Quercus* after 3940 cal yr BP. In Sierra de Baza, there was a replacement of mesophytic by more xeric taxa around 3800 cal yr BP (Carrión et al., 2007), while in El Cañizar de Villarquemado, mesophytes and deciduous *Quercus* decreased and steppe herbs increased between 4000-3800 cal yr BP. A similar pattern has been recorded in Italian sequences, with an expansion of sclerophyllous taxa between 3.9-3.4 ka (Sadori et al., 2010). These changes can all be attributed to both drier climate conditions and human activities, especially considering that several civilizations collapsed at ca. 4000 cal yr BP (i.e., Akkadians: Cullen et al., 2000; or Harappeans: An et al., 2005).

Peaks in *Artemisia* and high TIC percentages in BSM record mark two periods of increased aridity at 2.9-2.4, and at 1.2-0.7 cal ka BP (800-1300 AD). Both episodes are characterized by high TIC and TOC percentages and low TOC/TN ratios suggesting high precipitation of carbonates and high bioproductivity and content of autochthonous organic matter. These episodes are separated by a relative humid period between 2.1 and 1.5 cal ka BP. The arid phase between 2.9-2.4 ka cal BP is synchronous with a dry episode recorded in both western (Ferrio et al., 2006; Aguilera et al., 2012) and eastern Iberia, that led to a prominent decline in deciduous *Quercus* pollen in the Amposta sequence (Pérez-Obiol et al., 2011). Increased water level can be inferred from the significant reduction of TIC percentages between 2.1 and 1.5 cal ka BP. An episode of more humid conditions has been recognized in Iberia (Corella et al., 2010; Martín-

898 Puertas et al., 2008, 2009; Currás et al., 2012), coinciding with the Iberian civilization
899 and the Roman occupation and thus is called the Iberian-Roman Humid Period (IRHP).
900 The NW Mediterranean region also registers an intensification of rainfall reflected by
901 higher storm activity in the Gulf of Lion (Sabatier et al., 2012). However Fletcher et al.,
902 (2013b) report another phase of forest decline in Western Mediterranean at this time
903 (Fig. 5). Since wetter conditions should have positively affected forest development in
904 the Mediterranean, where water is the greatest limiting factor, it is possible that
905 depletion in tree mass could be related in some areas of Iberia to higher land use by the
906 Romans (García-Bellido, 1985). However, we do not observe great exploitation of the
907 subalpine belt at BSM suggesting that the vegetation composition, which runs in
908 parallel with sedimentological features, is still primarily controlled by climate.
909 The second arid period recorded in BSM sequence matches the well-known
910 Medieval Climate Anomaly (MCA: 900-1300 AD), a period of aridity recognized in
911 most of south-western Europe (Seager et al., 2007; Mann et al., 2009) which led to
912 notable agro-economic crisis in medieval societies. In Spain, it resulted in a major water
913 deficit leading to lower lake levels and expansion of thermophytes and steppe taxa
914 (Moreno et al., 2012b). In the BSM sequence, this phase coincides with the first signal
915 of deforestation, indicated by abrupt decreases in pine percentages. Charcoal influx
916 increased ca. 1700 cal BP, most likely because of either warmer conditions or
917 strengthened regional fire activity in the lowlands.
918 Both episodes of depleted water availability correspond with maxima in
919 reconstructed North Atlantic Oscillation (NAO) indexes (Fig. 5). This indicates that
920 there is a fast response of palaeoenvironmental changes in the BSM record to changes in
921 the North Atlantic. The persistence of a positive NAO index during 2.9-2.4, and at 1.2-
922 0.7 cal ka BP, led to maximum winter precipitation in Scandinavia and to minimum
923 winter precipitation in the Iberian Peninsula (Trouet et al., 2009).
924
925 **5.5. The last 8 centuries (Unit 1, BSM-V, CHZ-IV, 700 cal yr BP-present)**
926 In contrast to most Pyrenean studies that indicate intensified human disturbance
927 during at least the last two millennia (Riera et al., 2004; Pèlach et al., 2011; Guiter et al.,
928 2005), the effects of anthropogenic pressure are only detected in the BSM sequence
929 during the last 700 cal yr BP (Pérez-Sanz et al., 2011) (Fig, 6, BSM-V-A). As seen in
930 Figures 4, 5 and 6, the increase in *Olea* marks an expansion of agricultural practises in
931 the lowlands (Cañellas-Boltà et al., 2009) whereas large, short-term reductions in *Pine*

indicate phases of deforestation and expansion of grazing lands at higher altitudes (Fig. 6, BSM-V-B). Parallel to *Olea*, *Fraxinus* also spreads. *Fraxinus* has traditionally been used in the region for hedgerows (Gómez and Fillat, 1981). Its parallel expansion to *Olea* marks the regional establishment of modern and intense agro-pastoral activities. The drop in *Artemisia* synchronous with clear evidence of increasing anthropogenic pressure in the highlands supports the idea that *Artemisia* is not an indicator of human activities in the BSM sequence.

The expansion of *Olea* and *Fraxinus* ceased, and deforestation temporarily stopped, between 1600 and 1850 AD coinciding with the second half of the Little Ice Age. This interval is characterized by the coldest conditions in the southern Pyrenees (González-Trueba et al., 2008; Morellón et al., 2012). A sharp decrease in evergreen *Quercus* coincides with these colder conditions. The rapid recovery of pine after intervals of deforestation emphasizes the fact that human disturbance at high altitudes was not strong and climatic conditions were the main determinant of vegetation changes. High values of MS and strong negative correlation with TIC during this period (Fig. 6; BSM-V-C) indicate increased sediment delivery to the lake and decreased carbonate productivity, both indicative of higher lake levels and increased runoff. The abundance of allocthonous organic matter, shown by low TOC and high TOC/N ratios, also supports the inference of high sediment delivery from the catchment. Fire activity was high for most of this period, confirming the occurrence of either regional fires linked to husbandry or local fires correlated with the occasional pine deforestation (Lasheras-Álvarez et al., in press). Although it is difficult to distinguish between human and climate-induced fires in this period, all other records indicate an intensification of anthropogenic activities after 700 yrs BP. A general decrease in temperature coinciding with the Little Ice Age (LIA i.e. 1300-1850 AD) has been recorded throghout Europe. Higher storm activity occurred in the NW Mediterranean, (Sabatier el al., 2012) (Fig. 5) while stronger climatic variability has been recognised in Iberia, although generally cold and humid conditions dominated (Benito et al., 2003; Valero-Garcés et al., 2008; Morellón et al., 2012; Moreno et al, 2008, 2012b).

A significant expansion of *Olea* associated with a marked phase of deforestation of the pine forest occurred right after the LIA (1880 AD) (Fig. 6, BSM-V-D). The Industrial Revolution in the 17th century brought major advances in agricultural techniques that resulted in increased efficiency and production and led to increased supply of food and raw materials. As result of the improvement of the agricultural

966 sector the population rose and demographic pressure in the southern Pyrenees increased
967 up to its maximum at the end of 19th and the early 20th century (García-Ruiz and Valero-
968 Garcés, 1998).
969 After 1960 AD pine forest recovered, AP increased up to 65% and there was a
970 reduction in trees (*Olea, Fraxinus*) related to anthropogenic activities (Fig. 6, BSM-V-
971 E). During the mid-20th century, social and economic changes in Spain forced
972 population to migrate from villages into cities as the industrial sector developed. In
973 Spain, and more specifically in the southern Pyrenees, mass migration took place in the
974 last third of the 20th century, resulting in abandonment of the rural lands and gradual
975 recovery of forests (Lasanta-Martínez et al., 2005). We observe a steep drop in fire
976 activity during this phase, most likely as consequence of rural abandonment (Fig.6,
977 BSM-V-E). Geochemical proxies suggest a decrease of average lake level during the
978 last 50 years. TIC percentages reach the highest values of the entire sequence,
979 exceeding the values recorded during the MCA. Particularly high bioproductivity is
980 shown by high TOC values, along with TOC/TN ratios and an increase of macrophyte-
981 related taxa, such as *Corynoneura* and *Pentaneurini*, and especially *Psectrocladius* gr.
982 *limbatellus*. Increases in bioproductivity in the recent period may be linked to the
983 presence of cow stockbreeding near the lake. However, stockbreeding has taken place in
984 this area at least since the last century (Lucio, 1982) but the increase in bioproductivity
985 only occurs during the last 30 years. One possible explanation is that enhanced
986 bioproductivity during the last decades reflects increased water temperatures. A global
987 warming trend has been widely recognised over recent decades (IPCC, 2007) and an
988 increase in temperature is also evident in the Mediterranean area (Brunetti et al., 2004;
989 Vargas-Yáñez et al., 2008; Camuffo et al., 2010) and in north-eastern Spain (El Kenawy
990 et al., 2012). Climate change in the Mediterranean area involves not only increased
991 temperature but often decreased precipitation. A decrease in snowpack depth, snow
992 cover and direct precipitation has been detected in the southern Pyrenees during the
993 most recent period (López-Moreno 2005; López-Moreno and Stähli, 2008). The recent
994 drop in level at Basa de la Mora could be linked to the reduction in water availability in
995 the southern Pyrenees, while the increase in bioproductivity could be related to the
996 occurrence of warmer waters. The impact of the recent climate conditions on the lake
997 sediments confirms the high sensitivity and rapid response of Basa de la Mora record to
998 short-term climate shifts.
999

6.- CONCLUSIONS

The multi-proxy sequence of Basa de la Mora (BSM) has recorded significant climate variability during the last ca. 10 cal ka BP. Consistent shifts in vegetation, fire activity, depositional environments and aquatic communities throughout the sequence can be correlated with other regional and global reconstructions.

Higher seasonality between 10 and 8.2 cal ka BP caused high snow accumulation in winter and subsequent melt during warmer summers resulted in high lake levels. As a consequence of this high seasonal contrast, *Pinus* spread while mesophytes were restricted to watercourses. High climate instability during this period is illustrated by the occurrence of four short arid intervals at 9.7, 9.3, 8.8 and 8.3 cal ka BP, each characterized by a decrease in mesophytes and increased runoff. The most intense event occurred at 8.3 ± 0.1 cal ka BP, when vegetation diversity and abundance dropped to a minimum.

The most humid period in BSM sequence occurred between 8.2 and 5.7 cal ka BP. During this period, mesophytes expanded, conifers retreated and the highest lake level was recorded. As a consequence of increasing biomass, fire activity also intensified.

The end of the Mid-Holocene marks the transition from a significant Atlantic influence (before ca. 5.7 cal ka BP) into a typical Mediterranean climate with summer drought. A long-term trend towards increasing aridity, with decreasing lake levels and decreasing abundance of mesophytes started at 5.7 cal ka BP and intensified after ca. 3.9 cal ka BP. During this period and until 700 cal yr BP human exploitation of the subalpine belt was minor and the vegetation composition was primarily controlled by climate.

The BSM record shows that the Central Pyrenees are particularly sensitive to climate changes due to its geographical position between the Mediterranean and the Atlantic climate regimes.

7.- ACKNOWLEDGEMENTS

Financial support for research was provided by the former Spanish Inter-Ministry Commission of Science and Technology (CICIYT) through the projects DINAMO (CGL2009-07992), DINAMO2 (CGL2012-33063), GRACCIE-CONSOLIDER (CSD2007-00067) and HORDA (83/2008), from Parques Nacionales. Additional funding support has been provided by the Aragon Government through the project PM073/2007 and by Geoparque del Sobrarbe through the project "*High resolution chronological control of Basa de la Mora"*.

Ana Pérez-Sanz has been supported by a PhD Fellowship provided by the Aragon Government. Ana Moreno, Graciela Gil-Romera and Mario Morellón hold post-doctoral contracts funded by the "Ramón y Cajal", "Juan de la Cierva" and "JAE-DOC CSIC" programs, respectively. We thank to Santiago Giralt, Alberto Sáez, Armand Hernández, Carlos Martí, Mª Teresa Rico, Juan Pablo Corella and Antonio Vallejo for coring assistance in 2008. We also thank Beatriz Bueno and Aída Adsuar for their help in lab procedures. We are indebted to Prof. Sandy Harrison for her assistance with the English review that has led to a noticeable improvement of the manuscript.

References

Aguilera, M., Ferrio, J.P., Pérez, G., Araus, J.L., Voltas, J., 2012. Holocene changes in precipitation seasonality in the western Mediterranean Basin: a multi-species approach using δ13C of archaeobotanical remains. Journal of Quaternary Science 27, 192–202.

Ali, A.A., Carcaillet, C., Guendon, J., Quinif, Y., Roiron, P., Terral, J., 2003. The Early Holocene treeline in the southern French Alps: new evidence from travertine formations. Global Ecology and Biogeography 12, 411–419.

Alley, R., Agustsdottir, A., 2005. The 8k event: cause and consequences of a major Holocene abrupt climate change. Quaternary Science Reviews 24, 1123–1149.

Alley, R.B., Mayewski, P.A., Sowers, T., Stuiver, M., Taylor, K.C., Clark, P.U., 1997. Holocene climatic instability: A prominent, widespread event 8200 yr ago. Geology 25, 483-486.

Anderson, R.S., Jiménez-Moreno, G., Carrión, J.S., Pérez-Martínez, C., 2011. Postglacial history of alpine vegetation, fire, and climate from Laguna de Río Seco, Sierra Nevada, southern Spain. Quaternary Science Reviews 30, 1615–1629.

Appley P.G., 2001. Chronostratigraphic techniques in recent sediments. In: Last WM, Smol JP (eds) Tracking environmental change using lake sediments volume 1: basin analysis, coring, and chronological techniques. Kluwer, Dordrecht, pp 171–203

Bal, M.-C., Pelachs, A., Perez-Obiol, R., Julia, R., Cunill, R., 2011. Fire history and human activities during the last 3300cal yr BP in Spain's Central Pyrenees: The case of the Estany de Burg. Palaeogeography, Palaeoclimatology, Palaeoecology 300, 179–190.

Belmonte, A., 2004. La extensión máxima del glaciarismo en el Macizo de Cotiella (Pirineo Oscense). Boletín Glaciológico Aragonés 4, 69–90.

Benito, G., Sopeña, A., Sánchez-Moya, Y., Machado, M.J., Pérez-González, A., 2003. Palaeoflood record of the Tagus River (Central Spain) during the Late Pleistocene and Holocene. Quaternary Science Reviews 22, 1737–1756.

Bennett, K.D., 2009. Documentation for psimpoll 4.27 and pscomb 1.03. C programs for plotting and analyzing pollen data. The 14Chrono Centre, Archaeology and Palaeoecology, Queen's University of Belfast, Belfast, UK.

Bjune, A.E., Bakke, J., Nesje, A., Birks, H.J.B., 2005. Holocene mean July temperature and winter precipitation in western Norway inferred from palynological and glaciological lake-sediment proxies. The Holocene 15, 177–189.

Blarquez, O., Carcaillet, C., 2010. Fire, Fuel Composition and Resilience Threshold in Subalpine Ecosystem. PLoS ONE 5, e12480.

Blarquez, O., Carcaillet, C., Bremond, L., Mourier, B., Radakovitch, O., 2009. Trees in the subalpine belt since 11 700 cal. BP: origin, expansion and alteration of the modern forest. The Holocene 20, 139–146.

Bond, G., 1997. A Pervasive Millennial-Scale Cycle in North Atlantic Holocene and Glacial Climates. Science 278, 1257–1266.

Bond, G., Kromer, B., Beer, J., Muscheler, R., Evans, M.N., Showers, W., Hoffmann, S., Lotti-Bond, R., Hajdas, I., Bonani, G., 2001. Persistent Solar Influence on North Atlantic Climate During the Holocene. Science 294, 2130 –2136.

Bordon, A., Peyron, O., Lézine, A.-M., Brewer, S., Fouache, E., 2009. Pollen-inferred Late-Glacial and Holocene climate in southern Balkans (Lake Maliq). Quaternary International 200, 19–30.

1089 Brodersen, K.P., Odgaard, B.V., Vestergaard, O., Anderson, N.J., 2001. Chironomid
1090 stratigraphy in the shallow and eutrophic Lake Sobygaard, Denmark: chironomid-
1091 macrophyte co-occurrence. Freshwater Biology 46, 253–267.

1092 Brooks, S.J., Birks, H.J.., 2001. Chironomid-inferred air temperatures from Lateglacial and
1093 Holocene sites in north-west Europe: progress and problems. Quaternary Science Reviews
1094 20, 1723–1741.

1095 Brooks, S.J., Langdon, P.G., Heiri, O., Quaternary Research Association (Great Britain), 2007.
1096 The identification and use of Palaearctic Chironomidae larvae in palaeoecology. DRA
1097 Technical Guide No 10, Quaternary Research Association, London.

1098 Brunetti, M., Buffoni, L., Mangianti, F., Maugeri, M., Nanni, T., 2004. Temperature,
1099 precipitation and extreme events during the last century in Italy. Global and Planetary
1100 Change 40, 141–149.

1101 Cacho, I., Grimalt, J.O., Canals, M., Sbaffi, L., Shackleton, N.J., Schönfeld, J., Zahn, R., 2001.
1102 Variability of the western Mediterranean Sea surface temperature during the last 25,000
1103 years and its connection with the Northern Hemisphere climatic changes.
1104 Paleoceanography 16, 40-52.

1105 Camuffo, D., Bertolin, C., Barriendos, M., Dominguez-Castro, F., Cocheo, C., Enzi, S.,
1106 Sghedoni, M., Valle, A., Garnier, E., Alcoforado, M.-J., Xoplaki, E., Luterbacher, J.,
1107 Diodato, N., Maugeri, M., Nunes, M.F., Rodriguez, R., 2010. 500-year temperature
1108 reconstruction in the Mediterranean Basin by means of documentary data and
1109 instrumental observations. Climatic Change 101, 169–199.

1110 Cañellas-Boltà, N., Rull, V., Vigo, J., Mercadé, A., 2009. Modern pollen-vegetation
1111 relationships along an altitudinal transect in the central Pyrenees (southwestern Europe).
1112 The Holocene 19, 1185–1200.

1113 Carnelli, A.L., Theurillat, J.-P., Thinon, M., Vadi, G., Talon, B., 2004. Past uppermost tree limit
1114 in the Central European Alps (Switzerland) based on soil and soil charcoal. The Holocene
1115 14, 393–405.

1116 Carré, M., Azzoug, M., Bentaleb, I., Chase, B.M., Fontugne, M., Jackson, D., Ledru, M.-P.,
1117 Maldonado, A., Sachs, J.P., Schauer, A.J., 2012. Mid-Holocene mean climate in the south
1118 eastern Pacific and its influence on South America. Quaternary International 253, 55–66.

1119 Carrión, J.S., 2002. Patterns and processes of Late Quaternary environmental change in a
1120 montane region of southwestern Europe. Quaternary Science Reviews 21, 2047–2066.

1121 Carrión, J.S., Andrade, A., Bennett, K.D., Navarro, C., Munuera, M., 2001a. Crossing forest
1122 thresholds: inertia and collapse in a Holocene sequence from south-central Spain. The
1123 Holocene 11, 635–653.

1124 Carrión, J.S., Fernández, S., Jiménez-Moreno, G., Fauquette, S., Gil-Romera, G., González-
1125 Sampériz, P., Finlayson, C., 2010. The historical origins of aridity and vegetation
1126 degradation in southeastern Spain. Journal of Arid Environments 74, 731–736.

1127 Carrión, J.S., Fuentes, N., González-Sampériz, P., Sánchez Quirante, L., Finlayson, J.C.,
1128 Fernández, S., Andrade, A., 2007. Holocene environmental change in a montane region of
1129 southern Europe with a long history of human settlement. Quaternary Science Reviews
1130 26, 1455–1475.

1131 Carrión, J.S., Munuera, M., Dupre, M., Andrade, A., 2001b. Abrupt vegetation changes in the
1132 Segura Mountains of southern Spain throughout the Holocene. Journal of Ecology 89,
1133 783–797.

1134 Carrión, J.S., Sánchez-Gómez, P., Mota, J.F., Yll, R., Chaín, C., 2003. Holocene vegetation
1135 dynamics, fire and grazing in the Sierra de Gádor, southern Spain. The Holocene 13, 839–
1136 849.

Chung, F.H., 1974. Quantitative interpretation of X-ray diffraction patterns of mixtures. II. Adiabatic principle of X-ray diffraction analysis of mixtures. Journal of Applied Crystallography 7, 526–531.

Clark, J.S., 1988. Particle motion and the theory of charcoal analysis: source area, transport, deposition and sampling. Quaternary Research 30, 67–80.

Collins, P.M., Davis, B.A.S., Kaplan, J.O., 2012. The mid-Holocene vegetation of the Mediterranean region and southern Europe, and comparison with the present day. Journal of Biogeography 39, 1848–1861.

Colombaroli, D., Henne, P.D., Kaltenrieder, P., Gobet, E., Tinner, W., 2010. Species responses to fire, climate and human impact at tree line in the Alps as evidenced by palaeo-environmental records and a dynamic simulation model. Journal of Ecology 98, 1346–1357.

Colombaroli, D., Vanniere, B., Emmanuel, C., Magny, M., Tinner, W., 2008. Fire--vegetation interactions during the Mesolithic--Neolithic transition at Lago dell'Accesa, Tuscany, Italy. The Holocene 18, 679–692.

Colonese, A.C., Zanchetta, G., Fallick, A.E., Martini, F., Manganelli, G., Drysdale, R.N., 2010. Stable isotope composition of Helix ligata (Müller, 1774) from Late Pleistocene–Holocene archaeological record from Grotta della Serratura (Southern Italy): Palaeoclimatic implications. Global and Planetary Change 71, 249–257.

Corella, J.P., Moreno, A., Morellón, M., Rull, V., Giralt, S., Rico, M.T., Pérez-Sanz, A., Valero-Garcés, B.L., 2010. Climate and human impact on a meromictic lake during the last 6,000 years (Montcortès Lake, Central Pyrenees, Spain). Journal of Paleolimnology 46, 351–367.

Cortés Sánchez, M., Jiménez Espejo, F.J., Simón Vallejo, M.D., Gibaja Bao, J.F., Carvalho, A.F., Martinez-Ruiz, F., Gamiz, M.R., Flores, J.-A., Paytan, A., López Sáez, J.A., Peña-Chocarro, L., Carrión, J.S., Morales Muñiz, A., Roselló Izquierdo, E., Riquelme Cantal, J.A., Dean, R.M., Salgueiro, E., Martínez Sánchez, R.M., De la Rubia de Gracia, J.J., Lozano Francisco, M.C., Vera Peláez, J.L., Rodríguez, L.L., Bicho, N.F., 2012. The Mesolithic–Neolithic transition in southern Iberia. Quaternary Research 77, 221–234.

Court-Picon, M., Buttler, A., Debeaulieu, J., 2005. Modern pollen–vegetation relationships in the Champsaur valley (French Alps) and their potential in the interpretation of fossil pollen records of past cultural landscapes. Review of Palaeobotany and Palynology 135, 13–39.

Cullen, H.M., deMenocal, P.B., Hemming, S., Brown, F.H., Guilderson, T., Sirocko, F., 2000. Climate change and the collapse of the Akkadian empire: Evidence from the deep sea. Geology 28, 379–382.

Cunill, R., Soriano, J.-M., Bal, M.-C., Pèlachs, A., Pérez-Obiol, R., 2011. Holocene treeline changes on the south slope of the Pyrenees: a pedoanthracological analysis. Vegetation History and Archaeobotany 21, 373-384.

Currás, A., Zamora, L., Reed, J.M., García-Soto, E., Ferrero, S., Armengol, X., Mezquita-Joanes, F., Marqués, M.A., Riera, S., Julià, R., 2012. Climate change and human impact in central Spain during Roman times: High-resolution multi-proxy analysis of a tufa lake record (Somolinos, 1280m asl). Catena 89, 31–53.

David, F., 1993. Evolutions de la limite spérieure des arbres dans les Alpes francaise du nord depuis la fin des temps glaciaires. Université d'Aix-Marseille III, 94p.

Davis, B.A.S., Brewer, S., Stevenson, A.C., Guiot, J., 2003. The temperature of Europe during the Holocene reconstructed from pollen data. Quaternary Science Reviews 22, 1701–1716.

1185 Davis, P.T., Menounos, B., Osborn, G., 2009. Holocene and latest Pleistocene alpine glacier
1186 fluctuations: a global perspective. Quaternary Science Reviews 28, 2021–2033.

1187 De Beaulieu, J.-L., Miras, Y., Andrieu-Ponel, V., Guiter, F., 2005. Vegetation dynamics in
1188 north-western Mediterranean regions: Instability of the Mediterranean bioclimate. Plant
1189 Biosystems - An International Journal Dealing with all Aspects of Plant Biology 139,
1190 114–126.

1191 deMenocal, P., Ortiz, J., Guilderson, T., Adkins, J., Sarnthein, M., Baker, L., Yarusinsky, M.,
1192 2000. Abrupt onset and termination of the African Humid Period: Quaternary Science
1193 Reviews 19, 347–361.

1194 Domínguez-Villar, D., Wang, X., Cheng, H., Martín-Chivelet, J., Edwards, R.L., 2008. A high-
1195 resolution late Holocene speleothem record from Kaite Cave, northern Spain: δ18O
1196 variability and possible causes. Quaternary International 187, 40–51.

1197 Dupré, M., 1988. Palinología y paleoambiente. Nuevos datos españoles. Referencias. Serie de
1198 trabajos varios, S.I.P.,84.

1199 Ebbesen, H., Hald, M., Eplet, T.H., 2007. Lateglacial and early Holocene climatic oscillations
1200 on the western Svalbard margin, European Arctic. Quaternary Science Reviews 26, 1999–
1201 2011.

1202 El Kenawy, A., López-Moreno, J.I., Vicente-Serrano, S.M., 2012. Trend and variability of
1203 surface air temperature in northeastern Spain (1920–2006): Linkage to atmospheric
1204 circulation. Atmospheric Research 106, 159–180.

1205 Favilli, F., Cherubini, P., Collenberg, M., Egli, M., Sartori, G., Schoch, W., Haeberli, W., 2009.
1206 Charcoal fragments of Alpine soils as an indicator of landscape evolution during the
1207 Holocene in Val di Sole (Trentino, Italy). The Holocene 20, 67–79.

1208 Fernández, S., Fuentes, N., Carrión, J.S., González-Sampériz, P., Montoya, E., Gil, G., Vega-
1209 Toscano, G., Riquelme, J.A., 2007. The Holocene and Upper Pleistocene pollen sequence
1210 of Carihuela Cave, southern Spain. Geobios 40, 75–90.

1211 Ferrio, J.P., Alonso, N., Lopez, J.B., Araus, J.L., Voltas, J., 2006. Carbon isotope composition
1212 of fossil charcoal reveals aridity changes in the NW Mediterranean Basin. Global Change
1213 Biology 12, 1253–1266.

1214 Finné, M., Holmgren, K., Sundqvist, H.S., Weiberg, E., Lindblom, M., 2011. Climate in the
1215 eastern Mediterranean, and adjacent regions, during the past 6000 years – A review.
1216 Journal of Archaeological Science 38, 3153–3173.

1217 Fleitmann, D., Burns, S.J., Mangini, A., Mudelsee, M., Kramers, J., Villa, I., Neff, U., Al-
1218 Subbary, A.A., Buettner, A., Hippler, D., Matter, A., 2007. Holocene ITCZ and Indian
1219 monsoon dynamics recorded in stalagmites from Oman and Yemen (Socotra). Quaternary
1220 Science Reviews 26, 170–188.

1221 Fletcher, M.S., Moreno, P., 2012. Have the Southern Westerlies changed in a zonally symmetric
1222 manner over the last 14,000 years? A hemisphere-wide take on a controversial problem.
1223 Quaternary International 253, 32–46.

1224 Fletcher, W.J., Debret, M., Sanchez Goni, M.F., 2013b. Mid-Holocene emergence of a low-
1225 frequency millennial oscillation in western Mediterranean climate: Implications for past
1226 dynamics of the North Atlantic atmospheric westerlies. The Holocene 23, 153-166.

1227 Fletcher, W.J., Goñi, M.F.S., 2007. Orbital- and sub-orbital-scale climate impacts on vegetation
1228 of the western Mediterranean basin over the last 48,000 yr. Quaternary Research 70, 451–
1229 464.

1230 Fletcher, W.J., Sánchez Goñi, M.F., Allen, J.R.M., Cheddadi, R., Combourieu-Nebout, N.,
1231 Huntley, B., Lawson, I., Londeix, L., Magri, D., Margari, V., Müller, U.C., Naughton, F.,
1232 Novenko, E., Roucoux, K., Tzedakis, P.C., 2010a. Millennial-scale variability during the

1233 last glacial in vegetation records from Europe. Quaternary Science Reviews 29, 2839–
1234 2864.

1235 Fletcher, W.J., Sanchez Goñi, M.F., Peyron, O., Dormoy, I., 2010b. Abrupt climate changes of
1236 the last deglaciation detected in a Western Mediterranean forest record. Climate of the
1237 Past 6, 245–264.

1238 Fletcher, W.J., Zielhofer, C., 2013a. Fragility of Western Mediterranean landscapes during
1239 Holocene Rapid Climate Changes. Catena 103, 16-29.

1240 Franco Múgica, F., García Antón, M., Maldonado Ruiz, J., Morla Juaristi, C., Sainz Ollero, H.,
1241 2001. The Holocene history of Pinus forests in the Spanish Northern Meseta. The
1242 Holocene 11, 343–358.

1243 Franco-Mugica, F., Gómez-Manza, F., Maldonado, J., Morla, C., Postigo, J.M., 2000. El papel
1244 de los pinares en la vegetación holocnena de la Península Ibérica. Ecología 14, 61–67.

1245 Frigola, J., Moreno, A., Cacho, I., Canals, M., Sierro, F.J., Flores, J.A., Grimalt, J.O., Hodell,
1246 D.A., Curtis, J.H., 2007. Holocene climate variability in the western Mediterranean region
1247 from a deepwater sediment record. Paleoceanography 22. PA2209,
1248 doi:10.1029/2006PA001307

1249 García-Bellido, A., 1985. La Península Ibérica en los comienzos de su historia. Colegio
1250 universitario Ediciones Istmo, Madrid.

1251 García-Ruiz, J.M., Beguería, S., López-Moreno, J.I., Lorente, A., Seeger, M., 2001. Los
1252 recursos hídricos superficiales del Pirineo aragonés y su evolución reciente. (Surface
1253 wáter resources in the Aragonese Pyrenees and their recent evolution. Geoforma,
1254 Logroño, 191p.

1255 García-Ruiz, J.M., Puigdefábregas, J., Creus, J., 1985. Los recursos hídricos superficiales del
1256 Alto Aragón. Instituto de Estudios Altoaragoneses.

1257 García-Ruiz, J.M., Valero-Garcés, B.L., 1998. Historical geomorphic processes and human
1258 activites in the Central Spanis Pyrenees. Mountain Research and Development 18, 3009–
1259 320.

1260 Gil-Romera, G., González-Sampériz, P., Lasheras-Álvarez, L., Sevilla-Callejo, M., Moreno, A.,
1261 Valero-Garcés, B., López-Merino, L., Pérez-Sanz, A., Aranbarri, J., García-Prieto Fronce,
1262 E., Submitted. Long-term biomass-modulated fire dynamics at the Southern Pyrenees.
1263 Quaternary Research

1264 Gómez, D., Fillat, F., 1981. La cultura ganadera del fresno. Pastos 11, 295–302

1265 Gómez-Paccard, M., Larrasoaña, J.C., Sancho, C., Muñoz, A., McDonald, E., Rhodes, E.J.,
1266 Osácar, M.C., Costa, E., Beamud, E., 2013. Environmental response of a fragile, semiarid
1267 landscape (Bardenas Reales Natural Park, NE Spain) to Early Holocene climate
1268 variability: A paleo- and environmental-magnetic approach. Catena. 103, 30-43.

1269 González-Sampériz, P., Utrilla, P., Mazo, C., Valero-Garcés, B., Sopena, M., Morellón, M.,
1270 Sebastián, M., Moreno, A., Martínez-Bea, M., 2009. Patterns of human occupation during
1271 the early Holocene in the Central Ebro Basin (NE Spain) in response to the 8.2 ka climatic
1272 event. Quaternary Research 71, 121–132.

1273 González-Sampériz, P., Valero-Garcés, B.L., Moreno, A., Jalut, G., García-Ruiz, J.M., Martí-
1274 Bono, C., Delgado-Huertas, A., Navas, A., Otto, T., Dedoubat, J.J., 2006. Climate
1275 variability in the Spanish Pyrenees during the last 30,000 yr revealed by the El Portalet
1276 sequence. Quaternary Research 66, 38–52.

1277 González-Sampériz, P., Valero-Garcés, B.L., Moreno, A., Morellón, M., Navas, A., Machín, J.,
1278 Delgado-Huertas, A., 2008. Vegetation changes and hydrological fluctuations in the
1279 Central Ebro Basin (NE Spain) since the Late Glacial period: Saline lake records.
1280 Palaeogeography, Palaeoclimatology, Palaeoecology 259, 157–181.

González-Trueba, J.J., Moreno, R.M., Martinez de Pison, E., Serrano, E., 2008. `Little Ice Age' glaciation and current glaciers in the Iberian Peninsula. The Holocene 18, 551–568.

Gottfried, M., Pauli, H., Futschik, A., Akhalkatsi, M., Barančok, P., Benito Alonso, J.L., Coldea, G., Dick, J., Erschbamer, B., Fernández Calzado, M.R., Kazakis, G., Krajči, J., Larsson, P., Mallaun, M., Michelsen, O., Moiseev, D., Moiseev, P., Molau, U., Merzouki, A., Nagy, L., Nakhutsrishvili, G., Pedersen, B., Pelino, G., Puscas, M., Rossi, G., Stanisci, A., Theurillat, J.-P., Tomaselli, M., Villar, L., Vittoz, P., Vogiatzakis, I., Grabherr, G., 2012. Continent-wide response of mountain vegetation to climate change. Nature Climate Change 2, 111–115.

Greatbatch, R. J., 2000. The North Atlantic Oscillation. Stochastic Environmental Research and Risk Assessment 14, 213-242.

Guiter, F., Andrieu-Ponel, V., Digerfeldt, G., Reille, M., Beaulieu, J.-L., Ponel, P., 2005. Vegetation history and lake-level changes from the Younger Dryas to the present in Eastern Pyrenees (France): pollen, plant macrofossils and lithostratigraphy from Lake Racou (2000 m a.s.l.). Vegetation History and Archaeobotany 14, 99–118.

Haas, J.N., Richoz, I., Tinner, W., Wick, L., 1998. Synchronous Holocene climatic oscillations recorded on the Swiss Plateau and at timberline in the Alps. The Holocene 8, 301–309.

Heiri, O., Wick, L., Van Leeuwen, J.F.., Van der Knaap, W.O., Lotter, A.F., 2003. Holocene tree immigration and the chironomid fauna of a small Swiss subalpine lake (Hinterburgsee, 1515 m asl). Palaeogeography, Palaeoclimatology, Palaeoecology 189, 35–53.

Hély, C., Braconnot, P., Watrin, J., Zheng, W., 2009. Climate and vegetation: Simulating the African humid period. Comptes Rendus Geoscience 341, 671–688.

Hofmann, W., 1986. Chironomid analysis, in: Handbook of Holocene Paleoecology and Paleohydrology. Wiley and Sons, Chichester, pp. 715–727.

Hoffman, J.S, Carlson, E., Winsor, K., Klinkhammer, G.P., LeGrande, A.N., Andrews, J.T., Strasser, J.C., 2012. Linking the 8.2 ka event and its freshwater forcing in the Labrador Sea. Geophysical Research Letters, 39, L18703, doi:10.1029/2012GL053047.

IPCC, 2007. Climate Change 2007: impacts, adaptation and vulnerability., Contribution of working group II to the fourth assessment report of the intergovernmental panel on cliamte change. ed. Cambridge University Press, Reino Unido.

Jalut, G., Dedoubat, J.J., Fontugne, M., Otto, T., 2009. Holocene circum-Mediterranean vegetation changes: Climate forcing and human impact. Quaternary International 200, 4–18.

Jalut, G., Esteban Amat, A., Bonnet, L., Gauquelin, T., Fontugne, M., 2000. Holocene climatic changes in the Western Mediterranean, from south-east France to south-east Spain. Palaeogeography, Palaeoclimatology, Palaeoecology 160, 255–290.

Jiménez-Moreno, G., Anderson, R. S., 2012. Holocene vegetation and climate change recorded in alpine bog sediments from the Borreguilles de la Virgen, Sierra Nevada, southern Spain. Quaternary Research 77, 44–53.

Kaplan, M.R., Wolfe, A.P., 2006. Spatial and temporal variability of Holocene temperature in the North Atlantic region. Quaternary Research 65, 223–231.

Kobashi, T., Severinghaus, J.P., Brook, E.J., Barnola, J.M., Grachev, A.M., 2007. Precise timing and characterization of abrupt climate change 8200 years ago from air trapped in polar ice. Quaternary Science Reviews 26, 1212–1222.

Kröpelin, S., Verschuren, D., Lézine, A.-M., Eggermont, H., Cocquyt, C., Francus, P., Cazet, J.-P., Fagot, M., Rumes, B., Russell, J.M., Darius, F., Conley, D.J., Schuster, M., Von

Suchodoletz, H., Engstrom, D.R., 2008. Climate-Driven Ecosystem Succession in the Sahara: The Past 6000 Years. Science 320, 765 –768.

Lasanta-Martínez, T., Vicente-Serrano, S.M., Cuadrat-Prats, J.M., 2005. Mountain Mediterranean landscape evolution caused by the abandonment of traditional primary activities: a study of the Spanish Central Pyrenees. Applied Geography 25, 47–65.

Lasheras-Álvarez, L., Pérez-Sanz, A., Gil-Romera, G., González-Sampériz, P., Sevilla-Callejo, M., Valero-Garcés, B.L., in press. Historia del fuego y la vegetación en una secuenica holocena del Pirineo Central: La Basa de la Mora. Cuadernos de Investigación Geográfica

Leira, M., Santos, L., 2002. An early Holocene short climatic event in the northwest Iberian Peninsula inferred from pollen and diatoms. Quaternary International 93-94, 3–12.

Lionello, P., Malanotte-Rizzoli, P., Boscolo, R., Alpert, P., Artale, V., Li, L., Luterbacher, J., May, W., Trigo, R., Tsimplis, M., Ulbrich, U., Xoplaki, E., 2006. The Mediterranean climate: An overview of the main characteristics and issues, in: Developments in Earth and Environmental Sciences. Elsevier, pp. 1–26.

López-Merino, L., Cortizas, A.M., López-Sáez, J.A., 2010. Early agriculture and palaeoenvironmental history in the North of the Iberian Peninsula: a multi-proxy analysis of the Monte Areo mire (Asturias, Spain). Journal of Archaeological Science 37, 1978–1988.

López-Moreno, J.I., 2005. Recent variations of snowpack depth in the Central Spanish Pyrenees. Artic, Antartic, and Alpine Research 37, 253–260.

López-Moreno, J.I., Stähli, M., 2008. Statistical analysis of the snow cover variability in a subalpine watershed: Assessing the role of topography and forest interactions. Journal of Hydrology 348, 379–394.

Lucio, J.V., 1982. Estudio del Medio Físico del Sobrarbe. Aprovechamiento de los pastos estivales en el Valle de Gistain. Explotación actual y capacidad potencial. ICONA, Huesca.

Magny, M., De Beaulieu, J.-L., Drescher-Schneider, R., Vannière, B., Walter-Simonnet, A.-V., Miras, Y., Millet, L., Bossuet, G., Peyron, O., Brugiapaglia, E., Leroux, A., 2007. Holocene climate changes in the central Mediterranean as recorded by lake-level fluctuations at Lake Accesa (Tuscany, Italy). Quaternary Science Reviews 26, 1736–1758.

Magny, M., Vannière, B., Calo, C., Millet, L., Leroux, A., Peyron, O., Zanchetta, G., La Mantia, T., Tinner, W., 2011. Holocene hydrological changes in south-western Mediterranean as recorded by lake-level fluctuations at Lago Preola, a coastal lake in southern Sicily, Italy. Quaternary Science Reviews 30, 2459–2475.

Magyari, E.K., Chapman, J., Fairbairn, A.S., Francis, M., Guzman, M., 2012. Neolithic human impact on the landscapes of North-East Hungary inferred from pollen and settlement records. Vegetation History and Archaeobotany 21, 279–302.

Mann, M.E., Zhang, Z., Rutherford, S., Bradley, R.S., Hughes, M.K., Shindell, D., Ammann, C., Faluvegi, G., Ni, F., 2009. Global Signatures and Dynamical Origins of the Little Ice Age and Medieval Climate Anomaly. Science 326, 1256–1260.

Marshall, J., Kushnir, Y., Battisti, D., Chang, P., Czaja, A., Dickons, R., Hurrell, J., McCartney, M., Saravanan, R., Visbeck, M., 2002. North Atlantic climate variability: phenomena, impacts and mechanisms. International Journal of Climatology 21, 1863–1898.

Martín-Puertas, C., Valero-Garcés, B.L., Brauer, A., Mata, M.P., Delgado-Huertas, A., Dulski, P., 2009. The Iberian–Roman Humid Period (2600–1600 cal yr BP) in the Zoñar Lake varve record (Andalucía, southern Spain). Quaternary Research 71, 108–120.

1375 Martín-Puertas, C., Valero-Garces, B.L., Pilar Mata, M., Gonzalez-Samperiz, P., Bao, R.,
1376 Moreno, A., Stefanova, V., 2008. Arid and humid phases in southern Spain during the last
1377 4000 years: the Zonar Lake record, Cordoba. The Holocene 18, 907–921.

1378 Mayewski, P.A., 2004. Holocene climate variability. Quaternary Research 62, 243–255.

1379 Menking, K.M., Peteet, D.M., Anderson, R.Y., 2012. Late-glacial and Holocene vegetation and
1380 climate variability, including major droughts, in the Sky Lakes region of southeastern
1381 New York State. Palaeogeography, Palaeoclimatology, Palaeoecology 353-355, 45–59.

1382 Meyers, P.A., 2003. Applications of organic geochemistry to paleolimnological reconstructions:
1383 a summary of examples from the Laurentian Great Lakes. Organic Geochemistry 34,
1384 261–289.

1385 Millán, M.M., Estrela, M.J., Miró, J., 2005. Rainfall Components: Variability and Spatial
1386 Distribution in a Mediterranean Area (Valencia Region). Journal of Climate 18, 2682–
1387 2705.

1388 Miras, Y., Ejarque, A., Riera, S., Palet, J.M., Orengo, H., Eubab, I., 2007. Dynamique holocène
1389 de la végétation et occupation des Pyrénées andorranes depuis le Néolithique ancien,
1390 d'après l'analyse pollinique de la tourbière de Bosc dels Estanyons (2180 m, Vall del
1391 Madriu, Andorre). Comptes Rendus Palevol 6, 291–300.

1392 Montserrat-Martí, J., 1992. Evolución glaciar y postglaciar del clima y la vegetación en la
1393 vertiente sur del Pirineo: estudio palinológico., Monografías del Instituto Pirenaico de
1394 Ecología-CSIC. Zaragoza.

1395 Moore, P.D., Webb, J.A., 1978. An illustrated guide to pollen analysis. Hodder and Stoughton,
1396 London.

1397 Moore, P.D., Webb, J.A., Collinson, M.E., 1991. Pollen Analysis, Second. ed. Blackwell
1398 Scientifc Publications. Oxford.

1399 Morales-Molino, C., Postigo-Mijarra, J.M., Morla, C., Garcia-Anton, M., 2012. Long-term
1400 persistence of Mediterranean pine forests in the Duero Basin (central Spain) during the
1401 Holocene: The case of Pinus pinaster Aiton. The Holocene 22, 561–570.

1402 Morellón, M., Pérez-Sanz, A., Corella, J.P., Büntgen, U., Catalán, J., González-Sampériz, P.,
1403 González-Trueba, J.J., López-Sáez, J.A., Moreno, A., Pla-Rabes, S., Saz-Sánchez, M. á.,
1404 Scussolini, P., Serrano, E., Steinhilber, F., Stefanova, V., Vegas-Vilarrúbia, T., Valero-
1405 Garcés, B., 2012. A multi-proxy perspective on millennium-long climate variability in the
1406 Southern Pyrenees. Climate of the Past 8, 683–700.

1407 Morellón, M., Valero-Garcés, B., Moreno, A., González-Sampériz, P., Mata, P., Romero, O.,
1408 Melchor Maestro, Navas, A., 2008. Holocene palaeohydrology and climate variability in
1409 northeastern Spain: The sedimentary record of Lake Estanya (Pre-Pyrenean range).
1410 Quaternary International 181, 15–31.

1411 Morellón, M., Valero-Garcés, B., Vegas-Vilarrúbia, T., González-Sampériz, P., Romero, Ó.,
1412 Delgado-Huertas, A., Mata, P., Moreno, A., Rico, M., Corella, J.P., 2009. Lateglacial and
1413 Holocene palaeohydrology in the western Mediterranean region: The Lake Estanya record
1414 (NE Spain). Quaternary Science Reviews 28, 2582–2599.

1415 Moreno, A., López-Merino, L., Leira, M., Marco-Barba, J., González-Sampériz, P., Valero-
1416 Garcés, B.L., López-Sáez, J.A., Santos, L., Mata, P., Ito, E., 2011. Revealing the last
1417 13,500 years of environmental history from the multiproxy record of a mountain lake
1418 (Lago Enol, northern Iberian Peninsula). Journal of Paleolimnology 46, 327–349.

1419 Moreno, A., González-Sampériz, P., Morellón, M., Valero-Garcés, B.L., Fletcher, W.J., 2012.
1420 Northern Iberian abrupt climate change dynamics during the last glacial cycle: A view
1421 from lacustrine sediments. Quaternary Science Reviews 36, 139–153.

Moreno, A., Pérez, A., Frigola, J., Nieto-Moreno, V., Rodrigo-Gámiz, M., Martrat, B., González-Sampériz, P., Morellón, M., Martín-Puertas, C., Corella, J.P., Belmonte, Á., Sancho, C., Cacho, I., Herrera, G., Canals, M., Grimalt, J.O., Jiménez-Espejo, F., Martínez-Ruiz, F., Vegas-Vilarrúbia, T., Valero-Garcés, B.L., 2012b. The Medieval Climate Anomaly in the Iberian Peninsula reconstructed from marine and lake records. Quaternary Science Reviews 43, 16–32.

Moreno, A., Valero-Garcés, B.L., González-Sampériz, P., Rico, M., 2008. Flood response to rainfall variability during the last 2000 years inferred from the Taravilla Lake record (Central Iberian Range, Spain). Journal of Paleolimnology 40, 943–961.

Muñoz Sobrino, C., Ramil-Rego, P., Gómez-Orellana, L., 2007. Late Würm and early Holocene in the mountains of northwest Iberia: biostratigraphy, chronology and tree colonization. Vegetation History and Archaeobotany 16, 223–240.

Muñoz Sobrino, C., Ramil□rego, P., Gómez-Orellana, L., Varela, R.A.D., 2005. Palynological data on major Holocene climatic events in NW Iberia. Boreas 34, 381–400.

Nesje, A., Bjune, A.E., Bakke, J., Dahl, S.O., Lie, Ø., Birks, H.J.B., 2006. Holocene palaeoclimate reconstructions at Vanndalsvatnet, western Norway, with particular reference to the 8200 cal. yr BP event. The Holocene 16, 717–729.

O'Brien, S.R., Mayewski, P.A., Meeker, L.D., Meese, D.A., Twickler, M.S., Whitlow, S.I., 1995. Complexity of Holocene Climate as Reconstructed from a Greenland Ice Core. Science 270, 1962–1964.

Oldfield, F., 2005. Environmental change: key issues and alternative perspectives. Cambridge University Press, Cambridge, UK; New York.

Oldfield, F., Dearing, J.A., 2003. The role of human activities in past environmental change, in: Paleoclimate, Global Change and the Future, IGBP. Berlin, pp. 143–162.

Ortu, E., Peyron, O., Bordon, A., De Beaulieu, J.L., Siniscalco, C., Caramiello, R., 2008. Lateglacial and Holocene climate oscillations in the South-western Alps: An attempt at quantitative reconstruction. Quaternary International 190, 71–88.

Pantaleón-Cano, J., Yll, E.-I., Pérez-Obiol, R., Roure, J.M., 2003. Palynological evidence for vegetational history in semi-arid areas of the western Mediterranean (Almería, Spain). The Holocene 13, 109–119.

Pausas, J.G., Paula, S., 2012. Fuel shapes the fire-climate relationship: evidence from Mediterranean ecosystems. Global Ecology and Biogeography 21, 1074–1082.

Pèlachs, A., Julià, R., Pérez-Obiol, R., Soriano, J.M., Bal, M.-C., Cunill, R., Catalan, J., 2011. Potential influence of Bond events on mid-Holocene climate and vegetation in southern Pyrenees as assessed from Burg lake LOI and pollen records. The Holocene 21, 95 –104.

Pèlachs, A., Soriano, J.M., Nadal, J., Esteban, A., 2007. Holocene environmental history and human impact in the Pyrenees. Contributions to Science 3, 421–429.

Pérez-Obiol, R., Bal, M.-C., Pèlachs, A., Cunill, R., Soriano, J.M., 2012. Vegetation dynamics and anthropogenically forced changes in the Estanilles peat bog (southern Pyrenees) during the last seven millennia. Vegetation History and Archaeobotany 21, 385–396.

Pérez-Obiol, R., Jalut, G., Julia, R., Pelachs, A., Iriarte, M.J., Otto, T., Hernandez-Beloqui, B., 2011. Mid-Holocene vegetation and climatic history of the Iberian Peninsula. The Holocene 21, 75–93.

Pérez-Sanz, A., González-Sampériz, P., Valero-Garcés, B., Moreno, A., Morellón, M., Sancho, C., Belmonte, A., Gil-Romera, G., Sevilla, M., Navas, A., 2011. Clima y actividades humanas en la dinámica de la vegetación durante los últimos 2000 años en el Pirineo central: el registro palinológico de la Basa de la Mora (Macizo de Cotiella). Zubía 23, 17–38.

1470 Pla, S., Catalán, J., 2005. Chrysophyte cysts from lake sediments reveal the submillennial
1471 winter/spring climate variability in the northwestern Mediterranean region throughout the
1472 Holocene. Climate dynamics 24, 263–278.

1473 Prat, N., Real, M., Rieradevall, M., 1992. Benthos of Spanish lakes and reservoirs. Limnetica 8,
1474 221–229.

1475 Rasmussen, S.O., Vinther, B.M., Clausen, H.B., Andersen, K.K., 2007. Early Holocene climate
1476 oscillations recorded in three Greenland ice cores. Quaternary Science Reviews 26, 1907–
1477 1914.

1478 Reille, M., Lowe, J.L., 1995. Atlas. Pollen et spores d'Europe et d'Afrique du nord. Éditions du
1479 Laboratorie de botanique historique et palynologie, Marselle. 530p.

1480 Reimer, P.J., Baillie, M.G.L., Bard, E., Bayliss, A., Beck, J.W., Blackwell, P.G., Bronk
1481 Ramsey, C., Buck, C.E., Burr, G.S., Edwards, R.L., Friedrich, M., Grootes, P.M.,
1482 Guilderson, T.P., Hajdas, I., Heaton, T.J., Hogg, A.G., Hughen, K.A., Kaiser, K.F.,
1483 Kromer, B., McCormac, F.G., Manning, S.V., Reimer, R.W., Richards, D.A., Southon,
1484 J.R., Talamo, S., Turney, C.S.M., Van der Plicht, J., Weyhenmeyer, C.E., 2009.
1485 INTCAL09 and MARINE09 radiocarbon age calibration curves, 0-50,000 years cal. BP.
1486 Radiocarbon 51, 1111–1150.

1487 Renssen, H., Goosse, H., Fichefet, T., 2007. Simulation of Holocene cooling events in a coupled
1488 climate model. Quaternary Science Reviews 26, 2019–2029.

1489 Renssen, H., Seppä, H., Crosta, X., Goosse, H., Roche, D.M., 2012. Global characterization of
1490 the Holocene Thermal Maximum. Quaternary Science Reviews 48, 7–19.

1491 Renssen, H., Seppä, H., Heiri, O., Roche, D.M., Goosse, H., Fichefet, T., 2009. The spatial and
1492 temporal complexity of the Holocene thermal maximum. Nature Geoscience 2, 411–414.

1493 Riera, S., Wansard, G., Julià, R., 2004. 2000-year environmental history of a karstic lake in the
1494 Mediterranean Pre-Pyrenees: the Estanya lakes (Spain). Catena 55, 293–324.

1495 Rieradevall, M., Bonada, N., Prat, N., 1999. Community structure and water quality in the
1496 Mediterranean streams of a natural park (St. Llorenc del Munt, NE Spain). Limnetica 17,
1497 45–56.

1498 Rieradevall, M., Brooks, S.J., 2001. An identification guide to subfossil Tanypodinae larvae
1499 (Insecta: Diptera: Chironomidae) based on cephalic setation. Journal of Paleolimnology
1500 25, 81–99.

1501 Roberts, N., Eastwood, W.J., Kuzucuoglu, C., Fiorentino, G., Caracuta, V., 2011. Climatic,
1502 vegetation and cultural change in the eastern Mediterranean during the mid-Holocene
1503 environmental transition. The Holocene 21, 147–162.

1504 Rubiales, J.M., García-Amorena, I., Hernández, L., Génova, M., Martínez, F., Manzaneque,
1505 F.G., Morla, C., 2010. Late Quaternary dynamics of pinewoods in the Iberian Mountains.
1506 Review of Palaeobotany and Palynology 162, 476–491.

1507 Sabatier, P., Dezileau, L., Colin, C., Briqueu, L., Bouchette, F., Martinez, P., Siani, G., Raynal,
1508 O., Von Grafenstein, U., 2012. 7000years of paleostorm activity in the NW
1509 Mediterranean Sea in response to Holocene climate events. Quaternary Research 77, 1–
1510 11.

1511 Sadori, L., Jahns, S., Peyron, O., 2011. Mid-Holocene vegetation history of the central
1512 Mediterranean. The Holocene 21, 117–129.

1513 Sadori, L., Mercuri, A.M., Mariotti Lippi, M., 2010. Reconstructing past cultural landscape and
1514 human impact using pollen and plant macroremains. Plant Biosystems - An International
1515 Journal Dealing with all Aspects of Plant Biology 144, 940–951.

Saether, O.A., 1979. Chironomid communities as water quality indicators. Holartic Ecology 2, 65–74.

Sancho, C., Peña, J.L., Muñoz, A., Benito, G., McDonald, E., Rhodes, E.J., Longares, L.A., 2008. Holocene alluvial morphopedosedimentary record and environmental changes in the Bardenas Reales Natural Park (NE Spain). Catena 73, 225–238.

Schnurrenberger, D., Russell, J., Kelts, K., 2003. Classification of lacustrine sediments based on sedimentary components. Journal of Paleolimnology 29, 141–154.

Seager, R., Graham, N., Herweijer, C., Gordon, A.L., Kushnir, Y., Cook, E., 2007. Blueprints for Medieval hydroclimate. Quaternary Science Reviews 26, 2322–2336.

Seguret, M., 1972. Etude tectonique des nappes et seris décollées de la partie centrale du versant sud des Pyrénees. Caractère synsédimentaire, rôle de la compression et de lagravité, Publications USTELA. Série Géologie Structurale nº 2, Montpellier, 155 p.

Shuman, B., Bravo, J., Kaye, J., Lynch, J.A., Newby, P., Webb, T., 2001. Late Quaternary Water-Level Variations and Vegetation History at Crooked Pond, Southeastern Massachusetts. Quaternary Research 56, 401–410.

Spötl, C., Nicolussi, K., Patzelt, G., Boch, R., 2010. Humid climate during deposition of sapropel 1 in the Mediterranean Sea: Assessing the influence on the Alps. Global and Planetary Change 71, 242–248.

Stockmarr, J., 1971. Tablets with spores used in absolute pollen analysis. Pollen Spores 13, 614–621.

Stoll, H.M., Moreno, A., Mendez-Vicente, A., Gonzalez-Lemos, S., Jimenez-Sanchez, M., Dominguez-Cuesta, M.J., Edwards, R.L., Cheng, H., Wang, X., submitted. Growth rates of speleothems in NW Iberian Peninsula over the last two glacial cycles and relationship with climate. Quaternary Research

Talon, B., 2010. Reconstruction of Holocene high-altitude vegetation cover in the French southern Alps: evidence from soil charcoal. The Holocene 20, 35–44.

Tinner, W., Conedera, M., Ammann, B., Lotter, A.F., 2005. Fire ecology north and south of the Alps since the last ice age. The Holocene 15, 1214–1226.

Tinner, W., Hu, F.S., 2003. Size parameters, size-class distribution and area-number relationship of microscopic charcoal: relevance for fire reconstruction. The Holocene 13, 499–505.

Tinner, W., Hubschmid, P., Wehrli, M., Ammann, B., Conedera, M., 1999. Long-term forest fire ecology and dynamics in southern Switzerland. Journal of Ecology 87, 273–289.

Tinner, W., Lotter, A., 2001. Central European vegetation response to abrupt climate change at 8.2 ka. Geology 29, 551–554.

Trigo, R., Osborn, T., Corte-Real, J., 2002. The North Atlantic Oscillation influence on Europe: climate impacts and associated physical mechanisms. Climate Research 20, 9–17.

Trouet, V., Esper, J., Graham, N.E., Baker, A., Scourse, J.D., Frank, D.C., 2009. Persistent Positive North Atlantic Oscillation Mode Dominated the Medieval Climate Anomaly. Science 324, 78–80.

Valero-Garcés, B.L., González-Sampériz, P., Delgado-Huertas, A., Navas, A., Machín, J., Kelts, K., 2000. Lateglacial and Late Holocene environmental and vegetational change in Salada Mediana, central Ebro Basin, Spain. Quaternary International 73/74, 29–46.

Valero-Garcés, B.L., Moreno, A., 2011. Iberian lacustrine sediment records: responses to past and recent global changes in the Mediterranean region. Journal of Paleolimnology 46, 319–325.

Valero-Garcés, B.L., Moreno, A., Navas, A., Mata, P., Machín, J., Delgado Huertas, A., González Sampériz, P., Schwalb, A., Morellón, M., Cheng, H., Edwards, R.L., 2008. The Taravilla lake and tufa deposits (Central Iberian Range, Spain) as palaeohydrological and palaeoclimatic indicators. Palaeogeography, Palaeoclimatology, Palaeoecology 259, 136–156.

Vannière, B., Colombaroli, D., Chapron, E., Leroux, A., Tinner, W., Magny, M., 2008. Climate versus human-driven fire regimes in Mediterranean landscapes: the Holocene record of Lago dell'Accesa (Tuscany, Italy). Quaternary Science Reviews 27, 1181–1196.

Vargas-Yáñez, M., Jesús García, M., Salat, J., García-Martínez, M.C., Pascual, J., Moya, F., 2008. Warming trends and decadal variability in the Western Mediterranean shelf. Global and Planetary Change 63, 177–184.

Venables, W.N., Smith, D.M., R Development Core Team, 2008. An introduction to R notes on R, a programming environment for data analysis and graphics. Dept. of Statistics and Mathematics, Wirtschaftsuniversität Wien, Wien, Austria.

Vescovi, E., Ravazzi, C., Arpenti, E., Finsinger, W., Pini, R., Valsecchi, V., Wick, L., Ammann, B., Tinner, W., 2007. Interactions between climate and vegetation during the Lateglacial period as recorded by lake and mire sediment archives in Northern Italy and Southern Switzerland. Quaternary Science Reviews 26, 1650–1669.

Wanner, H., Beer, J., Bütikofer, J., Crowley, T.J., Cubasch, U., Flückiger, J., Goosse, H., Grosjean, M., Joos, F., Kaplan, J.O., Küttel, M., Müller, S.A., Prentice, I.C., Solomina, O., Stocker, T.F., Tarasov, P., Wagner, M., Widmann, M., 2008. Mid- to Late Holocene climate change: an overview. Quaternary Science Reviews 27, 1791–1828.

Wanner, H., Brönnimann, S., 2012. Is there a global Holocene climate mode? PAGES news 20, 44-45.

Wanner, H., Solomina, O., Grosjean, M., Ritz, S.P., Jetel, M., 2011. Structure and origin of Holocene cold events. Quaternary Science Reviews 30, 3109–3123.

Wiederholm, T., 1983. Chironomidae of the Holarctic region. Keys and diagnoses. Part I. Larvae, Wiederholm. ed. Museum of Zoology and Entomology, Lund University.

Zhao, C., Yu, Z., Ito, E., Zhao, Y., 2010. Holocene climate trend, variability, and shift documented by lacustrine stable-isotope record in the northeastern United States. Quaternary Science Reviews 29, 1831–1843.

FIGURES AND TABLES

Figure 1. a) Location map of Basa de la Mora Lake in central Pyrenees (Spain).
b) 3D regional vegetation map. In order to better discern the topography, the North is plotted at the bottom of the figure.

Figure 2. a) Age-depth model for the composite sequence of Basa de la Mora Lake based on 15 AMS ^{14}C dates and ^{210}Pb and ^{137}Cs activity at top.
b) 210Pb-based age model and 137Cs profile obtained for the top 50 cm.

Figure 3. Main sedimentological features, geochemical and physical properties of the Basa de la Mora sequence plotted in depth, indicating the location and results of radiocarbon dates, Facies 1 to 6 (see Table 2), identification and description of the Sedimentary units.

Figure 4. Pollen diagram of selected taxa from Basa de la Mora sequence, plotted in depth. Other Mesophytes curve groups *Alnus*, *Salix*, *Ulmus*, *Populus* and *Juglans* pollen types; Mediterranean shrubs groups *Pistacia*, *Rhamnus*, *Phillyrea*, *Buxus*, *Sambucus*, *Ephedra fragilis* and *E. distachya* pollen types; and Deciduous forest curve groups *Betula*, *Corylus*, *Fagus*, *Tilia*, deciduous *Quercus* and *Other Mesophytes* pollen types. As usually, AP includes all the arboreal taxa (trees and shrubs) and NAP the herbaceous component excluding aquatics and ferns.

Figure 5. Diagram plotted in age, including selected pollen taxa, geochemical parameters, chironomid taxa and microcharcoal influx curves of Basa de la Mora sequence compared to NAO summer insolation curve for latitude 24ºN, regional phases of deforestation (Fletcher et al., 2013b) and phases of increased storm activity (Sabatier et al., 2012) in the Western Mediterranean. Note: Orhocladiinae (s.t.) means sum of rheophilous (see page taxa). Blue horizontal bars represent humid phases whereas yellow and orange bands represent arid phases and further arid events respectively.

Figure 6. Comparison of selected curves (pollen –*Pinus*, Evergreen *Quercus, Fraxinus, Olea, Artemisia, Potamogeton*-, geochemical proxies-MS, TIC, TOC, TOC/N- and chironomids –*Psectrocladius* gr. *limbatellus*-) from Basa de la Mora sequence with

global and regional records (Estanya salinity (Morellón et al., 2011); NH temperature reconstruction (Mann et al., 2003) and Solar Irradiance (Sthinhiber et al., 2008)) for the last 750 years, indicating the main climate and historical periods and the interpretation of local land use. Bands in rose mark the intense periods of anthropogenic activities.

Table 1. AMS radiocarbon dates from core BSM08-1A-1U. Rejected dates are shown in italics.

Table 2. Facies description and interpreted depositional environment of BSM sequence.

Table 3. a) Correlation values between Magnetic Susceptibility and other geochemical parameters in the different sedimentary units.
b) Correlation between MS and pollen taxa in the different pollen zones.

1643 Table 1. AMS radiocarbon dates from core BSM08-1A-1U. Rejected dates are shown in
1644 italics.
1645

(b) Lab Code	Depth (cm)	Sample type	^{14}C age (yr BP)	Calibrated age, 2σ (yr cal BP)	Median probability (yr cal BP)
Poz-29744	60	Terrestrial macrorest	385 ± 30	426-507	456
Poz-35854	172	Terrestrial macrorest	1335 ± 30	1231-1304	1276
Poz-29745	230	Terrestrial macrorest	2100 ± 30	1995-2146	2072
Poz-35853	269	Terrestrial macrorest	2615 ± 30	2718-2777	2749
Poz-35852	337	Terrestrial macrorest	3200 ± 30	3368-3469	3419
Poz-35804	422	Terrestrial macrorest	3815 ±35	4089-4299	4206
Poz-29743	502	Terrestrial macrorest	5185 ± 35	5893-6002	5942
Poz-35803	562	Terrestrial macrorest	5840 ± 40	6533-6745	6657
Poz-35802	677	Terrestrial macrorest	6450 ± 40	7288-7430	7367
Poz-29746	795	charcoal	7330 ± 50	8014-8214	8125
Poz-35801	943	Terrestrial macrorest	7930 ± 50	8628-8983	8778
Poz-29747	1011	charcoal	7950 ± 50	8640-8990	8817
Poz-29779	1167	Terrestrial macrorest	8780 ± 50	9581-9941	9798
Poz-35856	*1198*	*Bulk sediment*	*10710 ± 60*	*12547-12743*	*12627*
152235	*1206*	*Pollen concentrates*	*13080 ± 100*	*15181-16476*	*15828*

1646
1647

1648 Table 2. Facies description and interpreted depositional environment of BSM sequence.

Facies	Facies description
Clastic, laminated facies	
1	Gray banded to laminated quartz and carbonate silts. Mostly composed by clay minerals (45 %), calcite (17 %) and, quartz (7 %) and low organic matter (<1%). High MS (100 SI). Laminated intervals are composed of up to 1 cm thick couplets of (1) black, carbonate silty-sands with high quartz content, abundant hematites, chlorite and maphic minerals and occasional terrestrial and macrophyte remains and (2) gray carbonate silts with lower silicate minerals content and rare organic matter.
2	Dark gray laminated carbonate silts. Mineralogical composition similar to Facies 1, but better laminated higher organic content (1-2 %) and lower MS (average 40 SI). Couplets composed of mm- thick laminae of (1) black, carbonate silty-sands with abundant terrestrial and macrophyte remains and (2) brown carbonate silts with less siliciclastic minerals and lower organic matter.
3	Light gray banded carbonate silts. Dominant carbonate content (TIC, X %; calcite, 40 %); quartz (6 %) and significant amounts of hematites, pyrite, clinochlorite, other maphic. Low organic matter (1%). Very high MS (>150 SI).
Interpretation	Clastic dominated deposition in distal, deeper setting. Laminated facies reflect flooding episodes reaching the centre of the lake. More abundant carbonate (Facies 3) or organic matter (Facies 2) reflects changes in watershed and littoral environments.
Carbonate and organic-rich facies	
4	Black, massive, carbonate silts. Composition is dominated by calcite (45 %), quartz (10 %), clay minerals (10 %) and organic matter (>2%) of terrestrial and macrophyte origin. Abundant pyrite and rare hematites. Low MS (25 SI). Occasional presence of pennate diatoms.
5	Light gray, massive, carbonate silts. Composition is dominated by calcite (70 %), with relatively low quartz and clay minerals (7 %) and organic matter (<2%); occasional pyrite and rare hematites. Low MS (25 SI). Organic matter is terrestrial, macrophyte and lacustrine origin. Mottling is common. Abundant gastropods and presence of pennate diatoms.
6	Light brown, banded, carbonate silts. Composition is dominated by calcite (30 %), clay minerals (15 %) and relatively low quartz (9 %) and organic matter (<2%) mostly terrestrial and macrophyte remains.
Interpretation	Carbonate dominated deposition in littoral environments with higher carbonate and organic productivity (Facies 5) deeper, with more frequent anoxic conditions (Facies 4) and transitional (Facies 6).

1649

1650

Table 3.

a) Correlation values between Magnetic Susceptibility and other geochemical parameters in the different sedimentary units.

	Unit 1 (0-93 cm)		**Unit 2 (93-491 cm)**		**Sub-unit 3a (491-690 cm)**		**Sub-unite 3b (690-1168)**	
	MS		MS		MS		MS	
	r	p	r	p	r	p	r	p
Si	0.726	**< 0.001**	0.546	**< 0.001**	0.146	0.148	-0.346	**< 0.001**
Ti	0.699	**< 0.001**	0.688	**< 0.001**	0.280	**0.005**	-0.388	**< 0.001**
Mn	0.688	**< 0.001**	0.545	**< 0.001**	0.543	**<0.001**	0.451	**< 0.001**
Fe	0.806	**< 0.001**	0.582	**< 0.001**	0.643	**< 0.001**	0.162	**0.013**
Ca	-0.660	**< 0.001**	-0.564	**< 0.001**	0.179	0.075	0.671	**< 0.001**
TIC	-0.700	**< 0.001**	-0.591	**< 0.000**	0.404	<**0.001**	0.689	**< 0.001**
TOC	-0.746	**< 0.001**	-0.409	**< 0.001**	-0.609	**< 0.001**	-0.494	**< 0.001**

b) Correlation between MS and pollen taxa in the different pollen zones.

	BSM III and BSM IV (93-491 cm)		BSM II(491-815 cm)		BSM I (815-1168 cm)	
	MS		MS		MS	
	r	p	r	p	r	p
Pinus	0.453	0.003	0.444	0.006	0.464	0.001
Juniperus	0.351	0.023	—	—	0.339	0.021
Betula	-0.573	< 0.001	—	—	-0.517	< 0.001
Corylus	—	—	—	—	-0.292	0.049
Tilia	—	—	-0.537	0.002	—	—
Dec. *Quercus*	—	—	-0.528	0.001	—	—
Quercus fag.	-0.401	0.009	—	—	-0.373	0.018
Ever. *Quercus*	-0.378	0.014	—	—	-0.505	< 0.001
Artemisia	—	—	-0.433	0.007	—	—
Cyperaceae	—	—	0.414	0.017	—	—
Myriophyllum	—	—	—	—	-0.592	< 0.001

Figure 1. a) Location map of Basa de la Mora Lake in central Pyrenees (Spain).
b) 3D regional vegetation map. In order to better discern the topography, the North is plotted at the bottom of the figure.

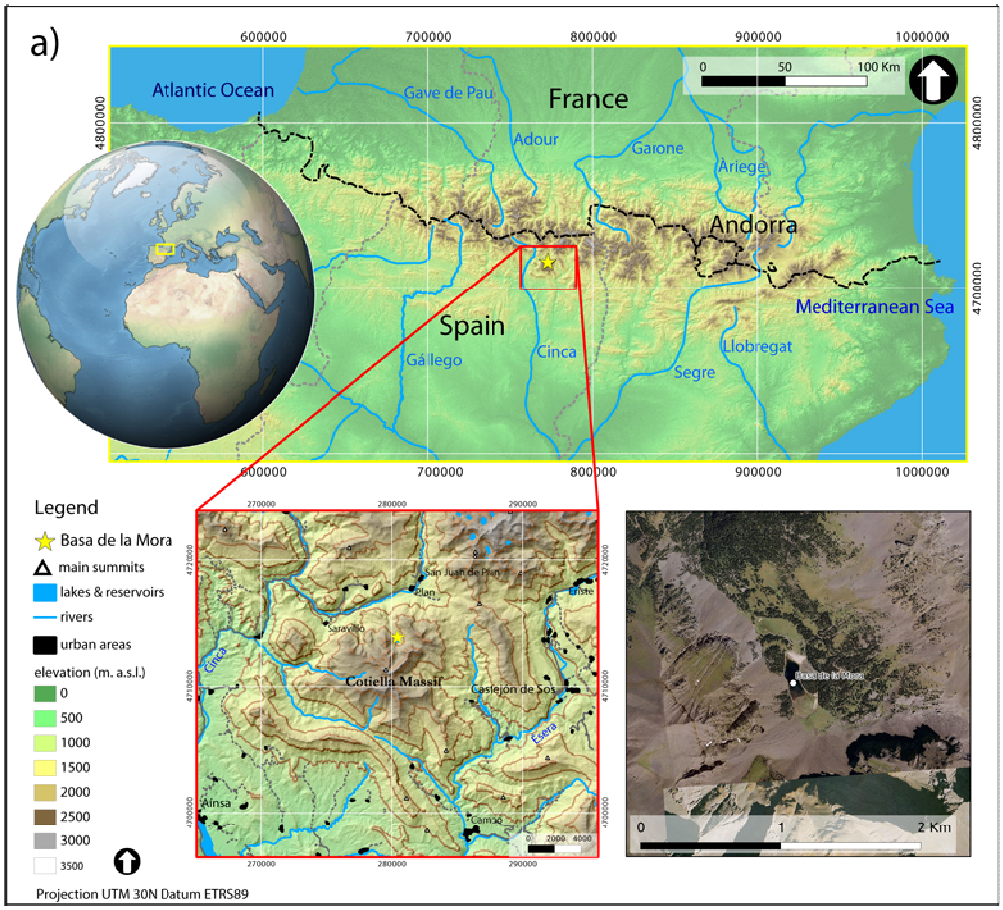

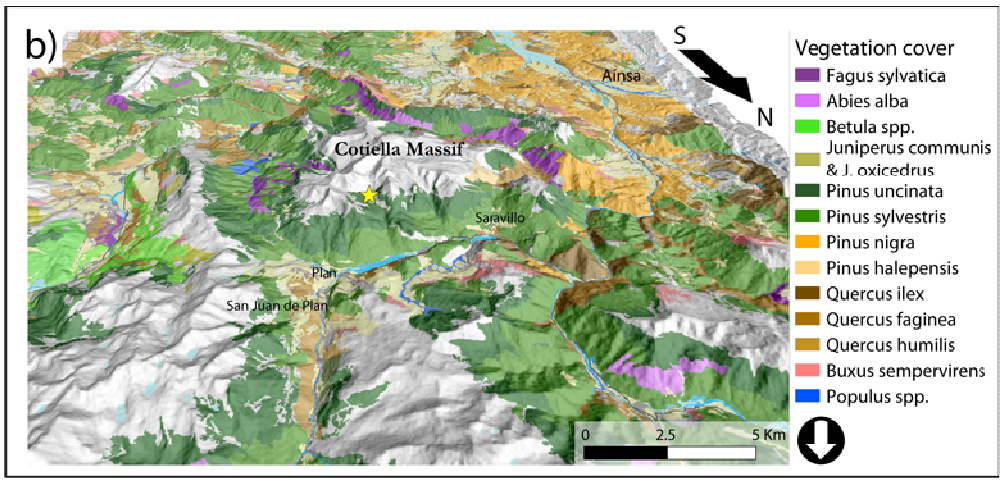

Figure 2. a) Age-depth model for the composite sequence of Basa de la Mora Lake based on 15 AMS ^{14}C dates and ^{210}Pb and ^{137}Cs activity at top.

b) 210Pb-based age model and 137Cs profile obtained for the top 50 cm.

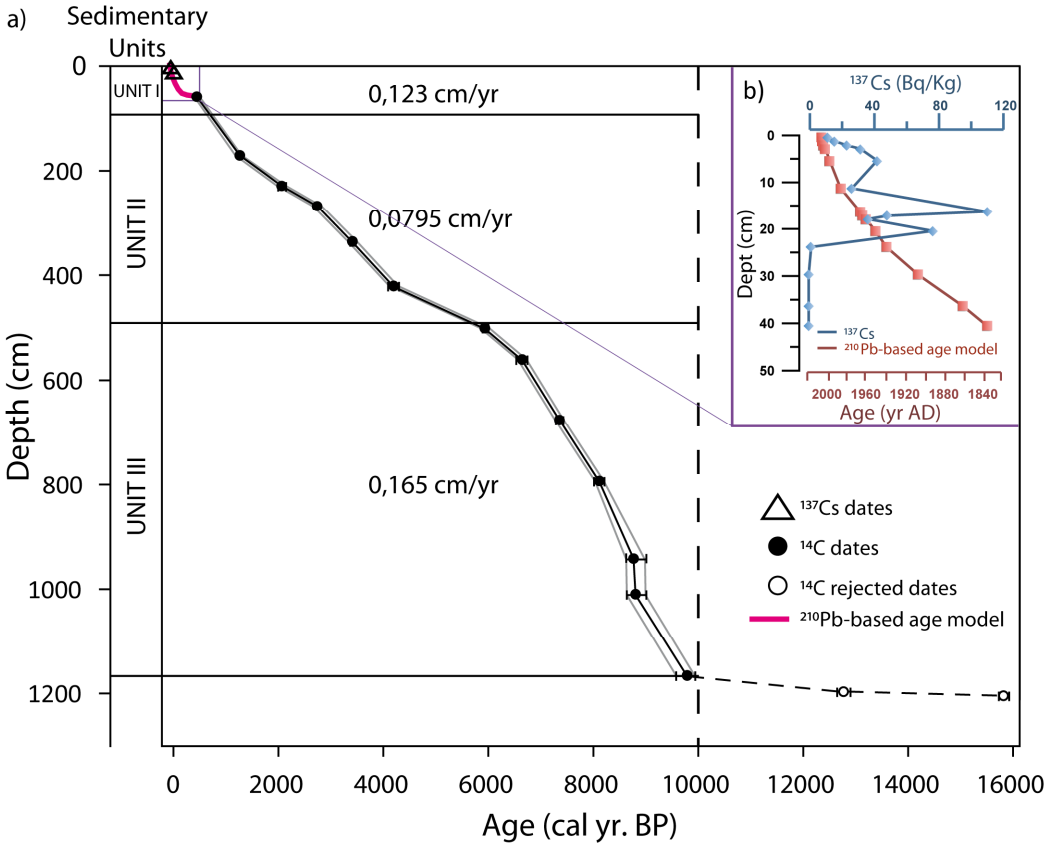

Figure 3. Main sedimentological features, geochemical and physical properties of the Basa de la Mora sequence plotted in depth, indicating the location and results of radiocarbon dates, Facies 1 to 6 (see Table 2), identification and description of the Sedimentary units.

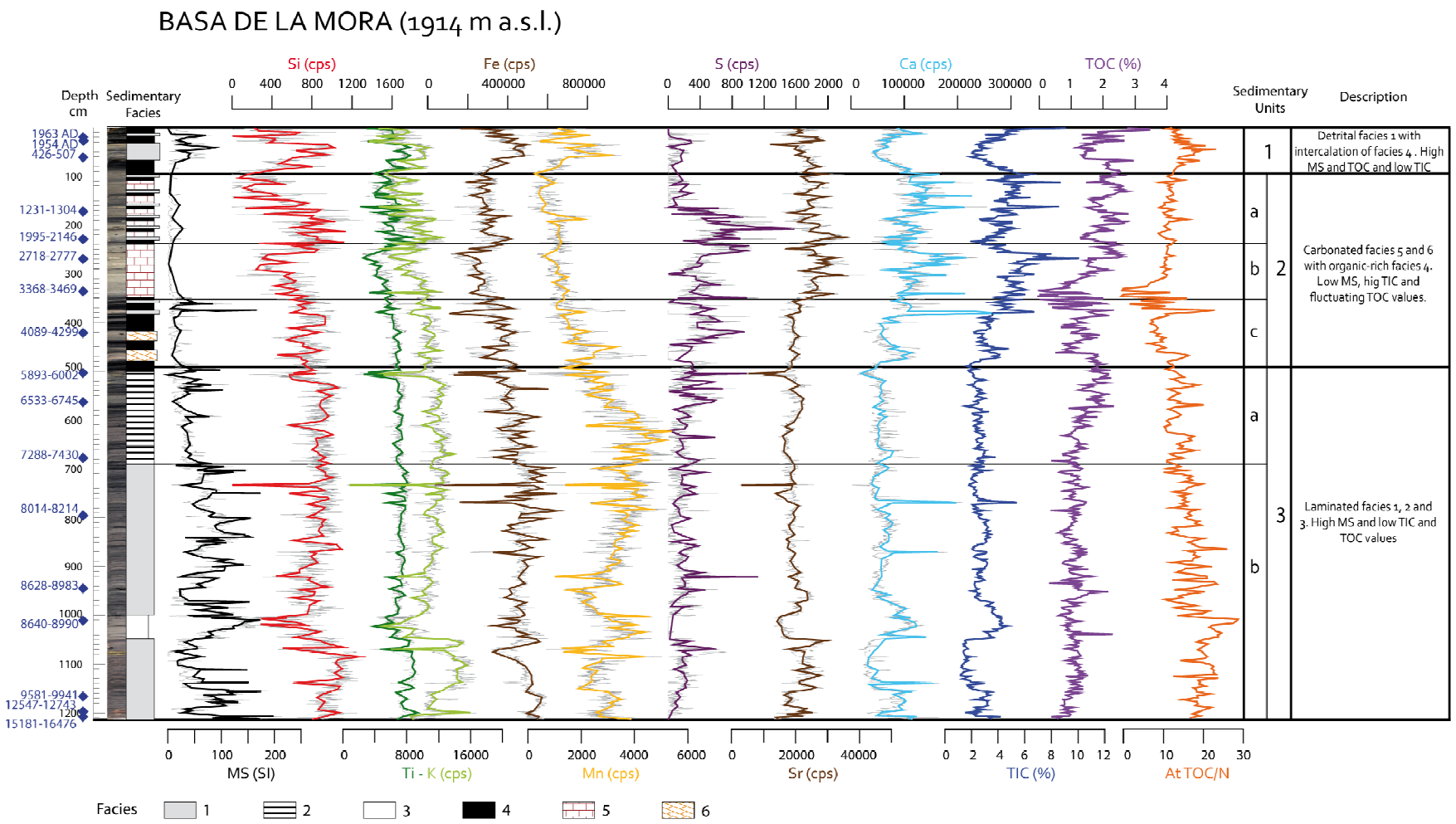

Figure 4. Pollen diagram of selected taxa from Basa de la Mora sequence, plotted in depth. Other Mesophytes curve groups *Alnus*, *Salix*, *Ulmus*, *Populus* and *Juglans* pollen types; Mediterranean shrubs groups *Pistacia*, *Rhamnus*, *Phillyrea*, *Buxus*, *Sambucus*, *Ephedra fragilis* and *E. distachya* pollen types; and Deciduous forest curve groups *Betula*, *Corylus*, *Fagus*, *Tilia*, deciduous *Quercus* and *Other Mesophytes* pollen types. As usually, AP includes all the arboreal taxa (trees and shrubs) and NAP the herbaceous component excluding aquatics and ferns.

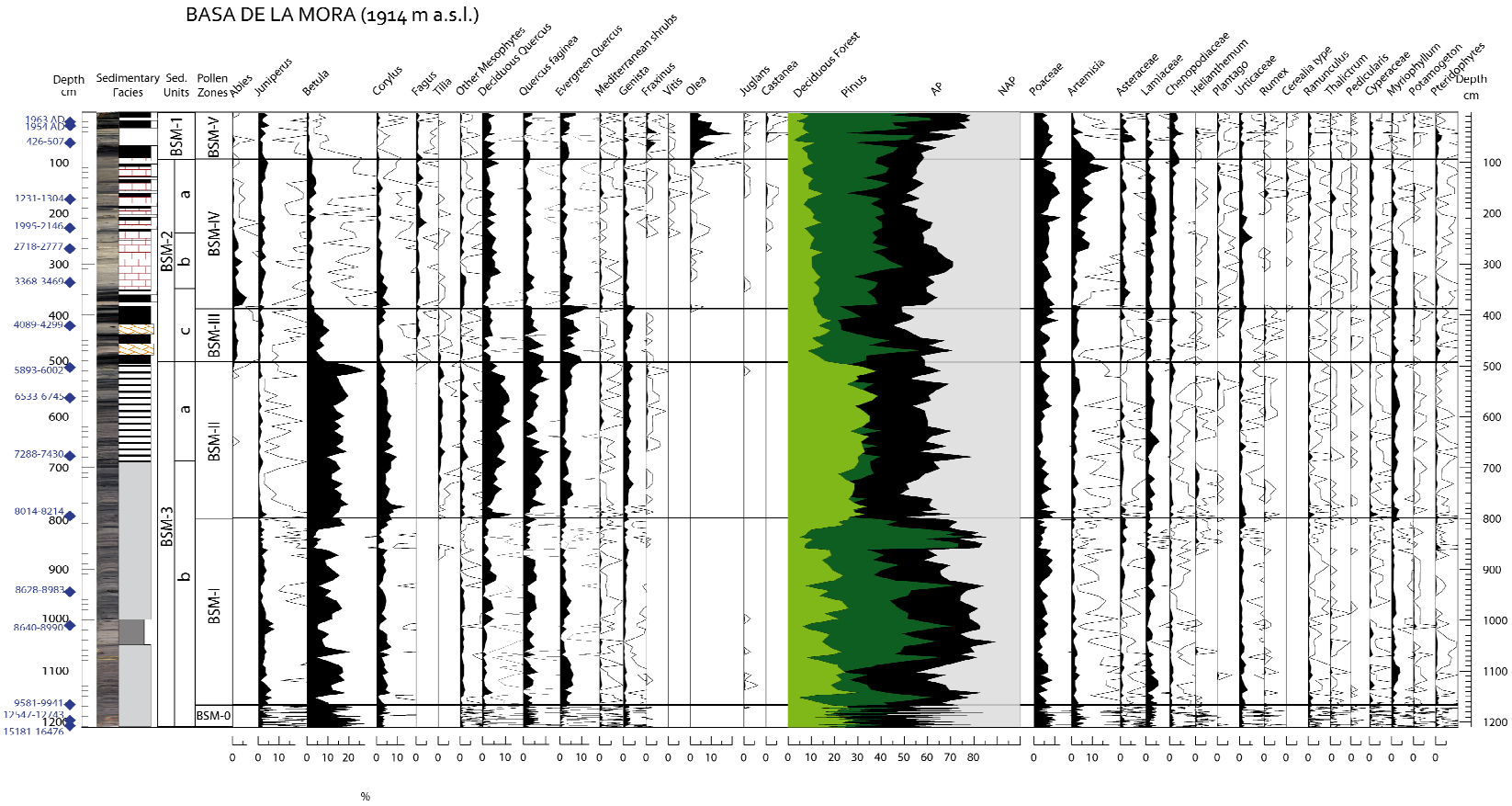

Figure 5. Diagram plotted in age, including selected pollen taxa, geochemical parameters, chironomid taxa and microcharcoal influx curves of Basa de la Mora sequence compared to NAO summer insolation curve for latitude 24ºN, regional phases of deforestation (Fletcher et al., 2013b) and phases of increased storm activity (Sabatier et al., 2012) in the Western Mediterranean. Note: Orhocladiinae (s.t.) means sum of rheophilous (see page taxa). Blue horizontal bars represent humid phases whereas yellow and orange bands represent arid phases and further arid events respectively.

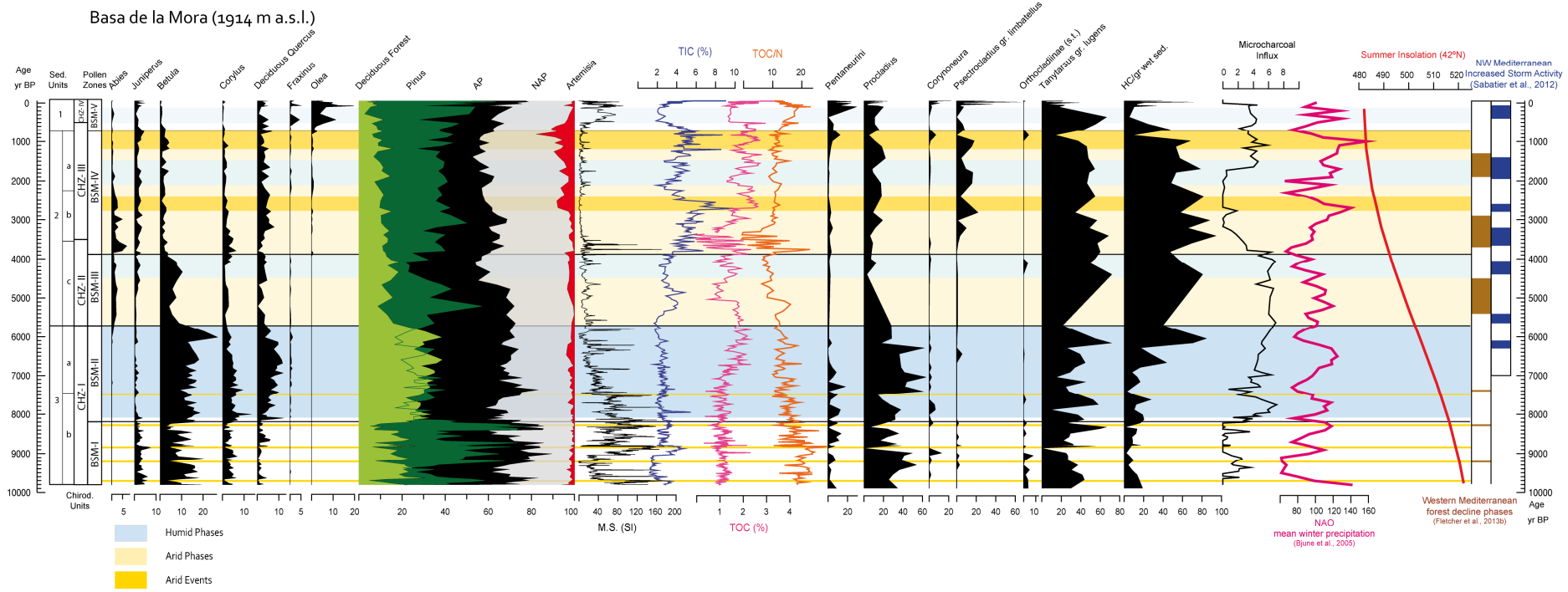

Figure 6. Comparison of selected curves (pollen –*Pinus*, Evergreen *Quercus, Fraxinus, Olea, Artemisia, Potamogeton*-, geochemical proxies- MS, TIC, TOC, TOC/N- and chironomids –*Psectrocladius* gr. *limbatellus*-) from Basa de la Mora sequence with global and regional records (Estanya salinity (Morellón et al., 2011); NH temperature reconstruction (Mann et al., 2003) and Solar Irradiance (Sthinhiber et al., 2008)) for the last 750 years, indicating the main climate and historical periods and the interpretation of local land use. Bands in rose mark the intense periods of anthropogenic activities.